Chemistry–A European Journal
Research Article
doi.org/10.1002/chem.202404778
Chemistry Europe
European Chemical Societies Publishing
www.chemeurj.org

Carbamate-Functionalized NLOphores via a Formal [2+2] Cycloaddition-Retroelectrocyclization Strategy

İpek Savaş,[a] Mehmet Efe Çelik,[a] Alberto Barsella,[b] and Cagatay Dengiz*[a]

This study introduces a new donor group capable of activating click-type [2+2] cycloaddition-retroelectrocyclizations, generally known for their limited scope. Target chromophores were synthesized using isocyanate-free urethane synthesis. The developed synthetic method allows for the tuning of the optical properties of the chromophores by modifying the donor groups, the acceptor units, and the side chains. The charge transfer (CT) bands of the chromophores exhibit λ_{max} values ranging from 363 to 692 nm. The CT bands observed have been supported by solvatochromism and protonation experiments. The synthesized compounds exhibit positive solvatochromism. Due to their potential as NLOphore candidates, the stability of the synthesized compounds have been investigated both experimentally through TGA and theoretically by calculating parameters such as frontier orbital energy differences, electronegativity, and global hardness/softness. TD-DFT calculations were used to elucidate the nature of the electronic transitions, revealing that the bands correspond to CT arising from HOMO-to-LUMO excitations. The NLO properties of the chromophores were investigated theoretically by DFT methods and experimentally by the EFISHG technique. Both results are shown to be in agreement with HOMO-LUMO energy differences. The experimental $\mu\beta$ values of the selected molecules range from 470×10^{-48} to 5400×10^{-48} esu.

Introduction

Intramolecular charge transfer (ICT) occurs when electronic charge shifts from an electron-rich donor site to an electron-deficient acceptor site within a single molecule.[1] Beyond its role in biological processes,[2] ICT is also crucial in the design of organic materials for advanced technologies. This includes applications in nonlinear optical (NLO) materials,[3] organic semiconductors,[4] organic light-emitting diodes (OLEDs),[5] dye-sensitized solar cells,[6,7] and fluorescence sensors.[8] Adjusting the ICT within a molecule can be used to fine-tune its linear and NLO responses.[1] Organic molecules with a "push-pull" structure, containing an electron donor (D) and an electron acceptor (A) connected by a π-bridge are typical platforms used in NLOphore synthesis due to their good ICT properties. An effective route to access D-π-A systems involves [2+2] cycloaddition-retroelectrocyclization (CA-RE) reactions.[9,10] These click-type reactions between electron-rich alkynes and electron-deficient alkenes, typically occurring under ambient conditions, have gained popularity in recent years because of their ability to efficiently link molecular units, their by-product-free nature, and their rapid reaction completion.[11] The reaction is considered to proceed in two stages: first, a formal [2+2] cycloaddition between an electron-rich alkyne and an electron-deficient olefin, followed by a retroelectrocyclization leading to the thermodynamically more stable butadiene derivatives.[12] However, the exact mechanism remains uncertain, with most of the literature suggesting a zwitterionic intermediate in the formation of the cyclobutene ring.[13] A recent study proposed an autocatalytic model, where the tetracyanobutadiene product is believed to serve as a template, helping to organize the reactants properly for the initial step of the [2+2] CA-RE cascade.[14] The success of these reactions largely depends on the specific structure of the alkenes and alkynes involved. The selection of alkenes is restricted to CN-substituted compounds, with tetracyanoethylene (TCNE) and 7,7,8,8-tetracyanoquinodimethane (TCNQ) being the most preferred choices due to their commercial availability.[9,15–27] The generation of toxic by-products like HCN during the synthesis of cyano-containing alkenes has redirected attention toward diversifying [2+2] CA-RE reactions through the synthesis of donor group-substituted alkynes. Beginning in 1981 with the use of metal acetylides[12] as electron-rich substrates, this method has enabled the development of various donor groups, including thiophene,[28] dialkylanilines,[29] anisole,[30] azulene,[31] ferrocene,[32] tetrathiafulvalene,[32] cyclopenta[*b*]furan-2-one,[33] porphyrin,[34] ynamides,[35] carbazole,[36] phenothiazine,[37] urea,[38] triazene,[39] *N*-alkylindole,[40] γ-pyranylidene,[41] and hydrazone.[42] Considering the applications of the non-planar push-pull chromophores obtained by [2+2] CA-RE in advanced technological fields,[9] the identification of new donor-substituted alkynes remains essential. Analysis using Hammett's substituent constants (σ) revealed that carbamates have more negative σ values compared to those of triazene-substituted aryl groups previ-

[a] İ. Savaş,+ M. E. Çelik,+ C. Dengiz
Department of Chemistry, Middle East Technical University, 06800 Ankara, Turkey
E-mail: dengizc@metu.edu.tr
[b] A. Barsella
Département d'Optique Ultra-Rapide et Nanophotonique, IPCMS-CNRS, 23 Rue du Loess, BP 43, 67034, Strasbourg, Cedex 2, France

Supporting information for this article is available on the WWW under https://doi.org/10.1002/chem.202404778

ously reported by our group, suggesting their potential as donor groups in [2 + 2] CA-RE.[43] Moreover, the recent study by Jayamurugan and co-workers[38] on utilizing urea as donor groups to activate alkynes in [2 + 2] CA-RE, along with the structural similarities between carbamates and urea, inspired us to pursue research in this area.

Carbamates with amide-ester hybrid structures experience resonance stabilization due to electron delocalization between nitrogen, oxygen lone pairs, and carbonyl groups.[44] This interaction results in highly rigid carbamate structures due to conformational restriction.[45] The polarity of a carbamate-containing molecules can be tailored by modifying the size, type, and substitution pattern of the aryl or alkyl groups, enabling precise control over the molecule's solubility and reactivity.[46] While carbamates play a significant role in drug discovery and medicinal chemistry,[44] their application in material science is relatively rare.[47] Hypothesizing that the bioactivity of carbamate-containing compounds stems from their ability to form charge transfer (CT) complexes with receptors, researchers investigated the formation of CT complexes with π-acceptors such as TCNE in experiments using *N*-arylcarbamates as donors.[48] Another key application of carbamates is their function as protecting groups, with *t*-butyloxycarbonyl (Boc) and carboxybenzyl (Cbz) being prime examples.[49] These materials also play a significant role in the polymer industry, with the most notable example being the use of polyurethanes containing carbamate functional groups. These are utilized in rigid foams for medical devices, footwear, coatings, adhesives, sealants, and as well as in automotive interior elastomers.[50] Besides, only a limited number of studies in the literature have explored the use of carbamates as ion sensors.[51] The most commonly used methods for synthesizing carbamates in the literature include the reductive carbonylation of aromatic nitro compounds,[52] Hoffmann rearrangement of amides,[53] Curtius rearrangement of acyl azides,[54] oxidative carbonylation[55] and phosgenation of amines.[56] Motivated by the lack of comprehensive studies on the donor properties of carbamates, this study examined the [2 + 2] CA-RE reactions of carbamate-substituted alkynes and TCNE/TCNQ.

Results and Discussion

Synthesis and Characterizations

Here, we presented the synthesis of a broad family of carbamate-substituted alkyne substrates and the corresponding push-pull chromophores obtained through click-type formal [2 + 2] CA-RE reactions of these substrates. In designing di-substituted alkyne substrates for formal [2 + 2] CA-RE reactions, six distinct arylcarbamate donors were employed to modify the structural characteristics, while five different donor, neutral, or acceptor groups were utilized to fine-tune their optical properties (Figure 1).

The initial set of substrates **1a–f**, selected for [2 + 2] CA-RE reactions to assess the donor properties of aryl carbamates, were designed to feature terminal alkynes (Scheme 1). With aryl carbamates being the sole functional group linked to the alkynes, the occurrence of the target reaction would validate the hypothesis regarding the donor characteristics of aryl carbamates. In the first step, aryl carbamates **8a–e** were synthesized in yields ranging from 78% to 99% by reactions of commercially available 4-iodoaniline (**6**) with different chloroformates **7a–e**. Subsequently, a Sonogashira cross-coupling reaction between carbamate-functionalized iodoarenes **8a–e** and trimethylsilylacetylene (TMSA) (**9**), followed by removal of the silyl protecting group from **10a–e**, gave the target alkynes **1a–e** in yields of 30–83%. Despite numerous attempts,

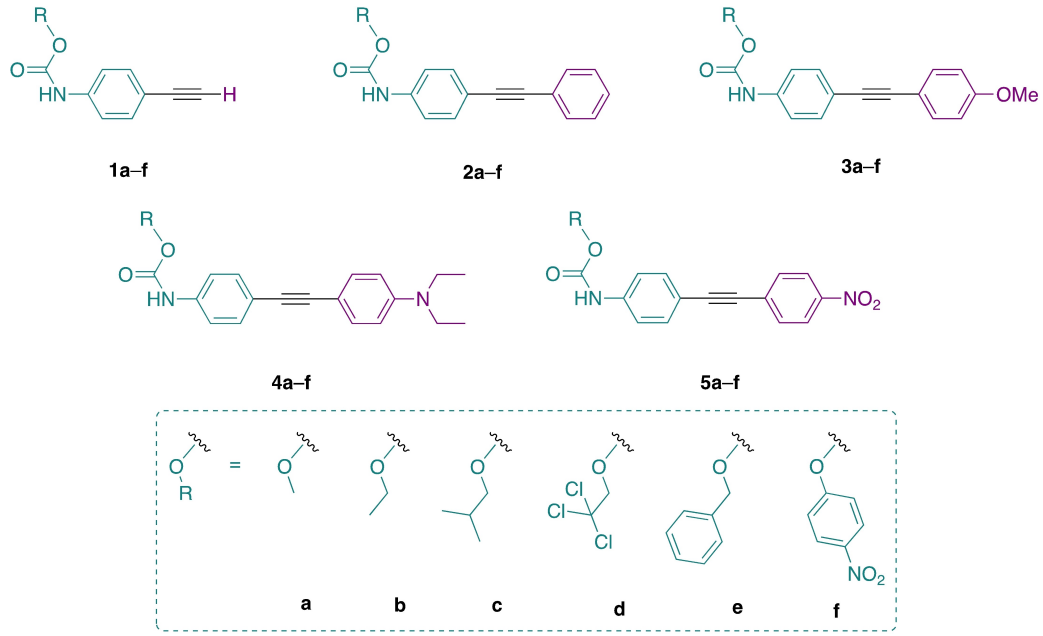

Figure 1. Designed carbamate-substituted alkynes.

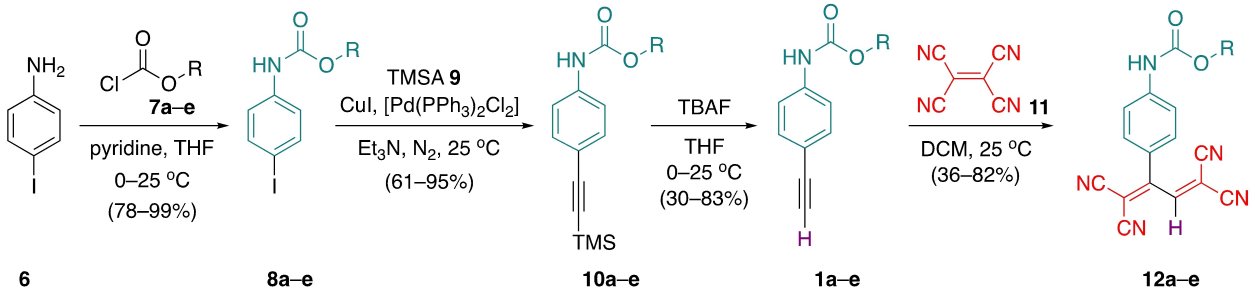

Scheme 1. [2 + 2] CA-RE reactions between alkynes **1a–e** and TCNE **11**.

compound **1f** with a nitrophenyl substituent could not be obtained due to stability issues. The electron-donating capacity of the carbamates was evaluated through [2 + 2] CA-RE between alkynes **1a–e** with the readily available electron-deficient olefin TCNE **11**. The successful synthesis of bright red chromophores **12a–e** indicated that the carbamate unit is a sufficient electron donor for [2 + 2] CA-RE cascades.

Recrystallization was employed for the isolation of chromophores **12a–e** during purification, as stability issues were encountered with column chromatography (SiO_2). In our recent study, we encountered a similar issue, which was resolved by using disubstituted alkynes in place of terminal alkynes.[42] In a similar approach, the terminal position of the alkyne was altered to include a phenyl ring to address this issue. During the initial attempt to synthesize the target substrates, the Sonogashira reactions of **8a–e** with phenylacetylene (**13**) yielded very low amounts, leading to a slight modification of the procedure (Scheme 2). Sonogashira cross-coupling reaction between 4-iodoaniline (**6**) and phenylacetylene (**13**) gave compound **14** in 80% yield. Following the cross-coupling, carbamate units were incorporated into the structures via chloroformates and **2a–f** were isolated in 56–90% yields. Unlike the terminal alkynes **1a–e**, compounds **2a–f** did not undergo [2 + 2] CA-RE spontaneously. A recent literature report demonstrated that structurally similar urea analogs were activated for [2 + 2] CA-RE using a Lewis acid mediators.[57] However, these conditions failed to yield a product for alkynes **2a–f**, leading to optimization of conditions for carbamate-containing structures. An inexpensive and readily available $LiClO_4$ was selected as the promoter due to its reported high efficiency in the cycloadditions of cyano-substituted olefins.[58]

The target chromophores **15a–e** were synthesized using modified methods, yielding between 50% and 96%. The reactions were carried out under reflux in acetonitrile with the assistance of $LiClO_4$ as a mediator. All transformations required elevated temperatures, and the low solubility of the obtained chromophores in common organic solvents made purification challenging, unlike the expected click-type conditions. The nitrophenyl-substituted analogue **15f** could not be synthesized due to the elimination of the carbamate group, resulting instead in the formation of the previously reported chromophore **16**[59], in 8% yield. The resulting chromophores **15a–e** were yellow, unlike the bright red TCBDs **12a–e** synthesized earlier. In contrast, chromophore **16** also exhibited a similar red color. The bulky phenyl group, which disrupts the planarity of the molecule, was considered a key factor in the reduced charge transfer and, consequently, the change in color. The color observed in compound **16** is thought to arise from the superior electron-donating ability of the free amine group compared to carbamates, owing to the lack of amide resonance. The acidic medium of silica cannot be tolerated by an electron-deficient carbamate **15f**, unlike the other carbamate derivatives **15a–e** which were successfully purified via column chromatography. The detachment trend for 4-nitrophenyl-substituted carbamate was not observed when in its alkyne form **2f**. This indicates that the partial positive charge on the carbonyl group was stabilized by the lone pairs on the N- and O-atoms, which aligns with its tolerance with column chromatography. How-

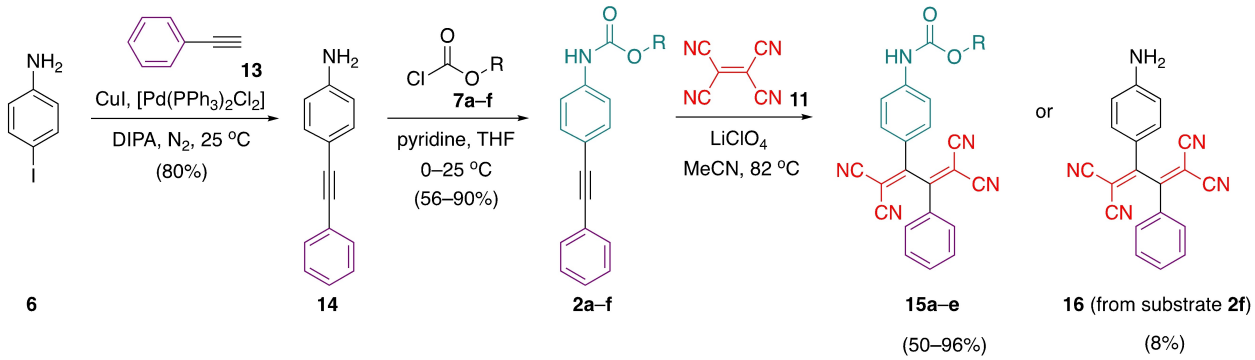

Scheme 2. Synthesis of phenyl-substituted chromophores **15a–e** and **16**.

ever, when the electron withdrawing TCBD structure is introduced, the lone pair on the nitrogen shifts to stabilize the more electron-deficient TCBD center. The substitution of the electron-deficient 4-nitrophenyl group directly into the extended resonance leaves the carbonyl center more positively charged and, therefore, more susceptible to nucleophilic attack, which we hypothesized occurs in the acidic environment of silica.

Replacing the phenyl group conjugated to the TCBD units with a stronger electron donor can reduce electron transfer from the carbamate to the TCBD unit, thereby enhancing the stability of the nitrophenyl-substituted chromophore structures. As a result, the anisole group was incorporated into the design. Following a similar approach to the synthesis of substrates **2a–f**, the **3a–f** series were synthesized via Sonogashira cross-coupling of 4-iodoaniline (**6**) with 1-ethynyl-4-methoxybenzene (**17**), followed by the reaction of the resulting aniline derivative **18** with chloroformates **7a–f**, yielding high yields ranging from 79% to 93% (Scheme 3). The alkynes **3a–f**, like the previous series **2a–f**, did not undergo [2+2] CA-RE without the presence of a Lewis acid. In reactions conducted with $LiClO_4$ in acetonitrile at 82 °C, carbamate-substituted chromophores **19a–e** were obtained in yields between 19% and 57%. However, the yield of compound **20**, resulting from the reaction of substrate **3f** with TCNE, was just 8%. These yields are relatively lower in comparison to those of phenyl-substituted chromophores **15a–e**. This outcome differs from literature findings, which indicate that a stronger donor substituent is expected to facilitate [2+2] CA-RE reactions more effectively, leading to higher yields.[9] We hypothesized that the coordination of the Lewis acid with methoxy group could account for the lower yields by reducing electron transfer from the methoxy group. Even though the desired chromophores **19a–e** were successfully obtained, the synthetic approach did not fully meet the intended click-type reaction conditions.

As a final attempt, the well-known electron-donor dialkylaniline was tested in an effort to achieve optimal click-type [2+2] CA-RE conditions (Scheme 4). In a similar approach to the synthesis of anisole-containing systems, the Sonogashira cross-coupling reaction between 4-iodoaniline (**6**) and 4-ethynyl-*N*,*N*-diethylaniline (**21**) was employed for the synthesis of substrate precursor **22**. In the following step, carbamate-functionalized alkynes **4a–f** were synthesized in 43–91% yields using different chloroformates. These alkynes successfully underwent [2+2] CA-RE with TCNE **11** without the need for Lewis acid mediation and also reacted under ideal click-type conditions, yielding high amounts and rapidly transforming into dark red chromophores **23a–e**. A similar trend of carbamate hydrolysis was also observed for alkyne **4f**, resulting in the formation of the amine-substituted chromophore **24** with an even increased yield (63%). These results indicate that, although we successfully induced carbamate-containing alkynes to undergo [2+2] CA-RE reactions under click-type conditions with strong donor groups, we were unable to reduce the charge transfer between the carbamate groups and TCBD units. Additionally, carbamate hydrolysis became more efficient in the presence of diethylaniline groups. We are actively pursuing further investigations to address this issue. At this stage, we speculate that the geometry of the structures formed after [2+2] CA-RE may better align the carbamate and conjugated dicyanovinyl units, facilitating more efficient intramolecular charge transfer. Based on these results, TCNQ, which is a comparatively bulkier electron acceptor than TCNE, was tested with substrates **1a–f**, **2a–f**, **3a–f**, and **4a–f**.

Even under Lewis acid-mediated conditions optimized for TCNE, substrates **1a–f**, **2a–f**, and **3a–f**, failed to undergo [2+2] CA-RE reactions with TCNQ. On the other hand, diethylaniline-activated alkynes **4a–e** smoothly participated in [2+2] CA-RE with TCNQ, yielding products **26a–e** in 78–94% yields. The reaction of the nitrophenyl-substituted substrate **4f** with TCNQ, like the reaction with TCNE, led to the elimination of the carbamate group, producing chromophore **27** in a 59% yield. The donor capacity of the proposed carbamate unit was last evaluated by replacing the aromatic ring attached to the alkyne unit with an electron-withdrawing group. The alkynes **5a–e** were synthesized from corresponding terminal alkynes **1a–e** in moderate yields (47–76%) (Scheme 5). Unfortunately, the [2+2] CA-RE of alkynes **5a–e** with TCNE did not proceed under ambient conditions or even at elevated temperatures mediated by Lewis acids. This concluded that the donating ability of the carbamates was insufficient to activate the alkynes for [2+2]

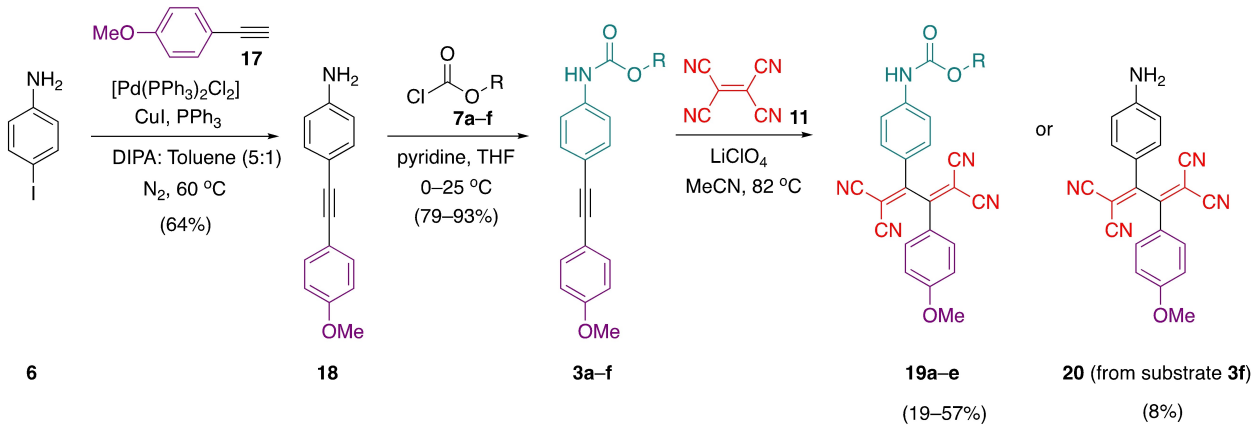

Scheme 3. Synthesis of anisole-substituted chromophores **19a–e** and **20**.

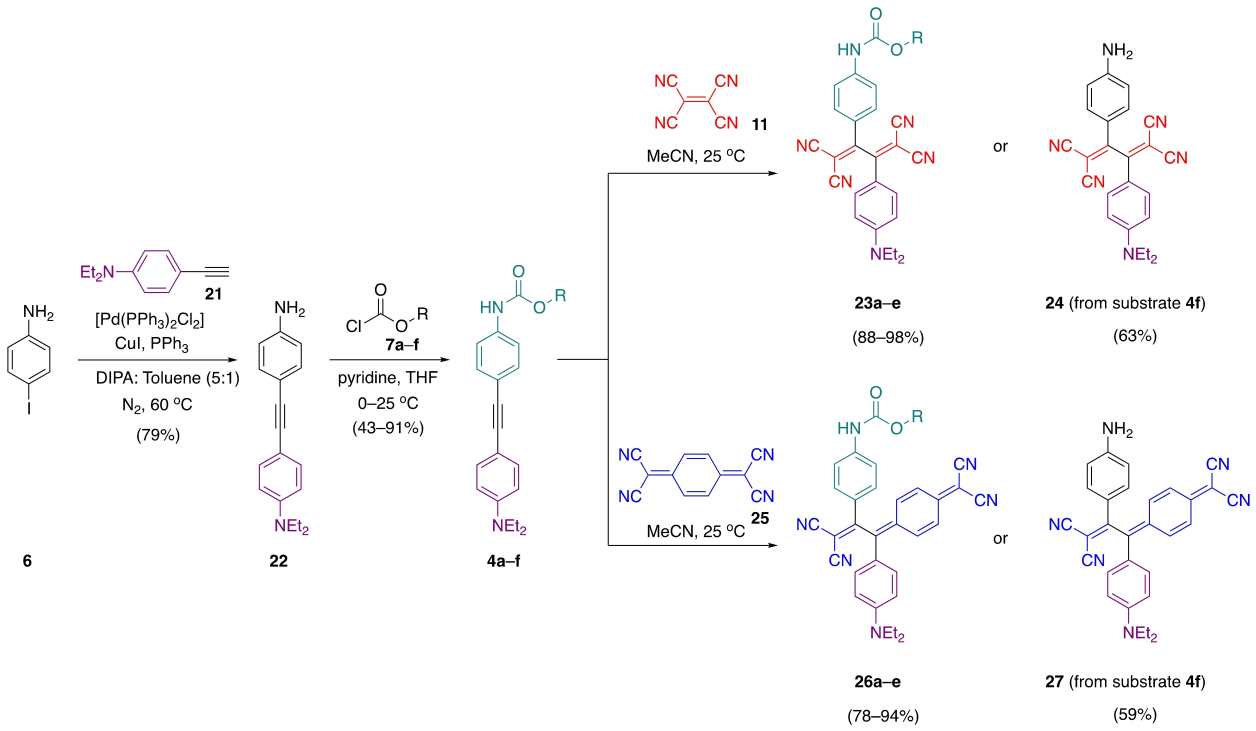

Scheme 4. Synthesis of diethylaniline-substituted chromophores **23a–e**, **24**, **26a–e**, and **27**.

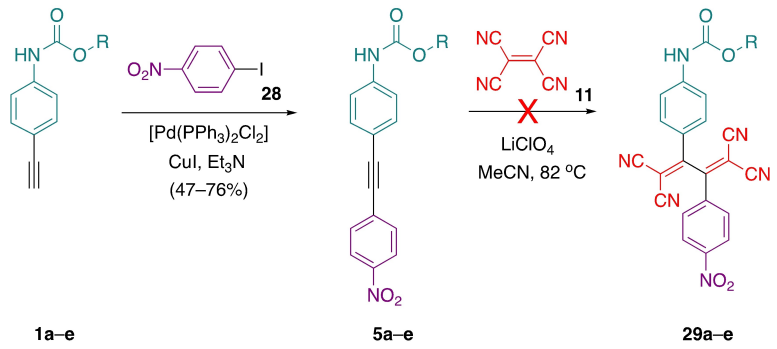

Scheme 5. Attempts towards the synthesis of nitrophenyl-substituted chromophores **29a–e**.

CA-RE when an electron-withdrawing group was already present in the molecule.

UV/Vis Spectroscopy

The light absorption characteristics of the reported chromophores have been studied via UV/Vis spectroscopy [Figure 2 and Figures S259–263 in the Supporting Information (SI)]. When comparing different carbamate moieties while keeping the rest of the molecule unchanged, it was found that altering the carbamate substituent had no significant electronic effect on the synthesized chromophores, as indicated by their similar absorption maxima values (Figures S259–263 in the SI). However, the versatility in derivatization and tolerance to various substituents [Figure 1; including alkyl chains (a, b, and c), 2,2,2-trichloroethyl (d), benzyl (e), and nitrophenyl (f)] were demonstrated by the number of chromophores successfully synthesized. A comparative UV/Vis spectrum for the representative isobutylcarbamate-substituted chromophores **12c**, **15c**, **19c**, **23c**, and **26c** were chosen due to the superior solubility of these compounds compared to other chromophores (Figure 2). The UV/Vis absorption spectrum of **12c** offers clear insight into the donor properties of the carbamate groups. The lowest energy absorption band at 447 nm, corresponding to intramolecular CT from the carbamate unit to the TCBD moiety, is consistent with the typical characteristics of CT bands. The phenyl-substituted yellow chromophore **15c** exhibits a hypsochromically shifted absorption maximum at 386 nm and a slightly lower molar extinction coefficient of 2.11×10^4 $M^{-1}cm^{-1}$, which correlates the phenyl group's interference in electron mobility within the chromophore due to deviation from planarity. By replacing phenyl group with an electron-donating methoxy unit, the orange chromophore **19c** exhibits an

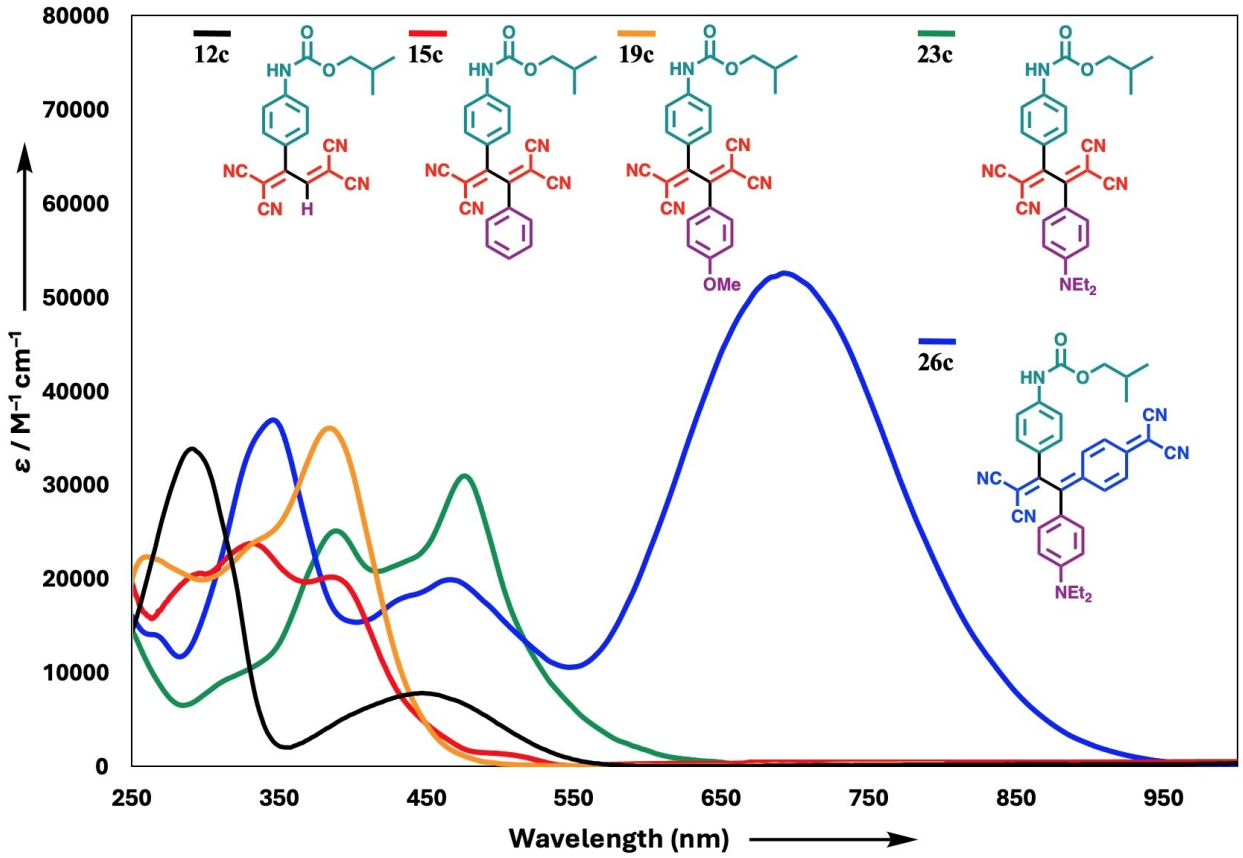

Figure 2. UV-Vis spectra of isobutyl carbamate-substituted chromophores **12c**, **15c**, **19c**, **23c**, and **26c**.

absorption maximum at 384 nm and a molar extinction coefficient of 3.61×10^4 $M^{-1}cm^{-1}$. The presence of the electron-donating methoxy benzene group resulted in a 1.5-fold increase in the extinction coefficient compared to the phenyl-substituted chromophore. The diethylaniline-substituted chromophore **23c**, which serves as a relatively stronger donor group than methoxy benzene, displays two distinct CT bands. These bands arise from two separate charge transfer pathways: one through the carbamate and the other through diethylaniline. A comparison of the methoxybenzene- and diethylaniline-substituted chromophores **19c** and **23c** reveals that the former has a higher extinction coefficient than the latter, likely due to the overlap of two distinct CT bands. Particularly, chromophore **26c** exhibits a significant bathochromic shift, with its absorption maximum at 692 nm. The extinction coefficient of the lowest energy absorption band for **26c** (5.26×10^4 $M^{-1}cm^{-1}$) indicates that this group of chromophores is highly suited for organic electronic applications, as it exhibits strong absorption over a large portion of the UV/Vis spectrum with high attenuation.

Solvatochromism is a routinely employed technique for assessing the CT properties of organic dyes.[60] Dyes with significant CT character typically display bathochromic (red) shifts in polar solvents, as the polar environment stabilizes the charge-separated state. The representative chromophore **26c** exhibited positive solvatochromism in different mixtures of CH_2Cl_2 and *n*-hexane (Figure 3). The CT nature of the lowest energy absorption band for the representative chromophore **26a** was further validated through a protonation experiment (Figure 4). When trifluoroacetic acid was added, this band disappeared due to the quaternization of the diethyl aniline group. However, the band fully reappeared after neutralization with triethylamine.

Thermal Gravimetric Analysis (TGA)

The literature widely acknowledges that thermal stability of chromophores is crucial for ensuring the long-term performance and reliability of devices used in NLO applications.[61] Considering the laser-induced heating in NLO applications and the high-temperature demands during processing of synthesized chromophores, NLOphores are expected to exhibit thermal stability above 200 °C.[62–64] Failure to meet these requirements often leads to reduced optical performance and changes in the material's nonlinear response. Thermogravimetric analysis (TGA) is a technique used to evaluate a material's thermal stability by monitoring changes in its mass as temperature is gradually increased under controlled laboratory conditions. To assess the thermal stability of our synthesized structures, we conducted TGA experiments at a heating rate of 10 °C/min, selecting two representative compounds **23d** and **26d** (Figure 5). While **23d** begins to lose mass at around 105 °C,

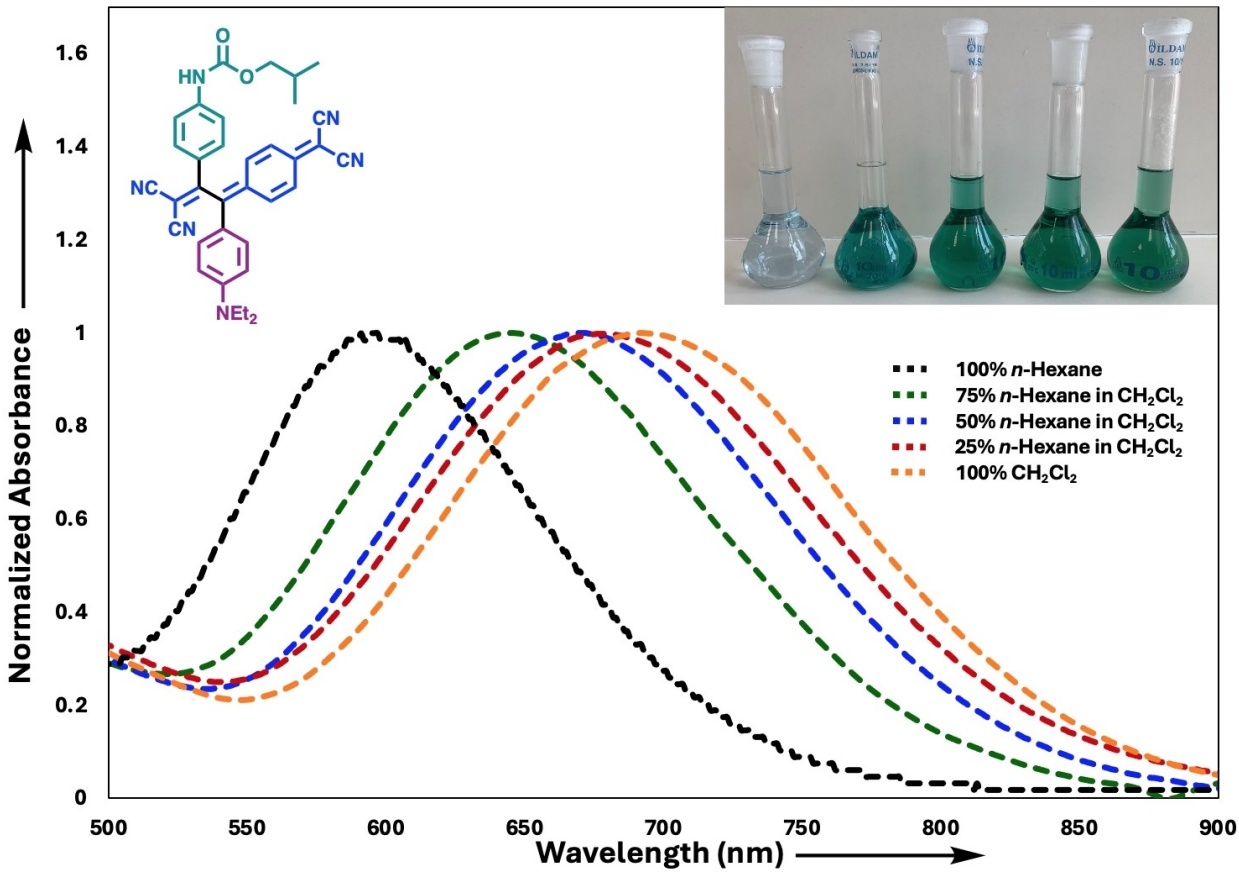

Figure 3. UV/Vis spectra of **26 c** in CH_2Cl_2/*n*-hexane mixtures at 25 °C.

26 d remains stable with minimal mass loss up to 200 °C. In a comparison emphasizing the 50% mass loss to highlight the thermal stability difference between the two compounds, **26 d** reaches 50% mass loss at 878 °C, whereas **23 d** achieves this point at 633 °C. These findings suggest that **26 d**, with a stronger electron-withdrawing group, is significantly more thermally stable than **23 d**. These results are consistent with findings reported in the literature[65,66] for similar systems, showing that the thermal stability of compound **26 d**, which would typically decrease with increased conjugation, is maintained due to its increased molar mass compared to **23 d**.

Computational Studies

Computational methods were employed to provide deeper insights into the experimental results related to the optical properties of the synthesized carbamate-substituted chromophores. This section primarily focuses on calculated energy level diagrams, TD-DFT calculations (Tables S1–S12 and Figure S265 in the SI), visualizations of frontier orbitals and ESP maps, stability parameters, and NLO calculations. Following conformational searches, only conformations within 3 kcal of the global minimum were selected for the subsequent Density Functional Theory (DFT) calculations. The aforementioned DFT calculations were carried out using the Gaussian09 software package at the CAM–B3LYP/6-31G++(d,p) level of theory, incorporating CPCM solvation in DCM and $CHCl_3$.[67] While the energies of the Highest Occupied Molecular Orbital (HOMO) and Lowest Unoccupied Molecular Orbital (LUMO) calculated using DFT methods are often considered inaccurate,[68] they still offer valuable insights into the reactivity and optical properties of chromophore structures. To address this, frontier orbital energy levels were determined using two different methods. The first approach calculates the direct energy gap between the HOMO and LUMO of the optimized structures (ΔE^{direct}), while the second approach uses the vertical excitation energy corresponding to the lowest singlet excited state (ΔE^{TD}). As anticipated, the energy range calculated using the first method is overestimated (**23 a–e**, **24**: 4.82–4.99 eV; **26 a–e**, **27**: 3.84–3.92 eV, Table 2), whereas the second method provides values more consistent with the UV/Vis results (**23 a–e**, **24**: 2.74–2.88 eV; **26 a–e**, **27**: 2.03–2.08 eV) (Figure 6). Nevertheless, both methods align in capturing the trend in frontier orbital energy ranges for the compound groups synthesized with TCNE and TCNQ. Specifically, the chromophores derived from TCNQ exhibit lower energy ranges compared to those obtained from TCNE. This can be attributed to the proaromatic nature of the quinone unit in **26 a–e** and **27**, as well as the improved ICT enabled by the extended conjugation.

In the following phase, HOMO, LUMO, and ESP map visualizations were analyzed to better understand the ICT

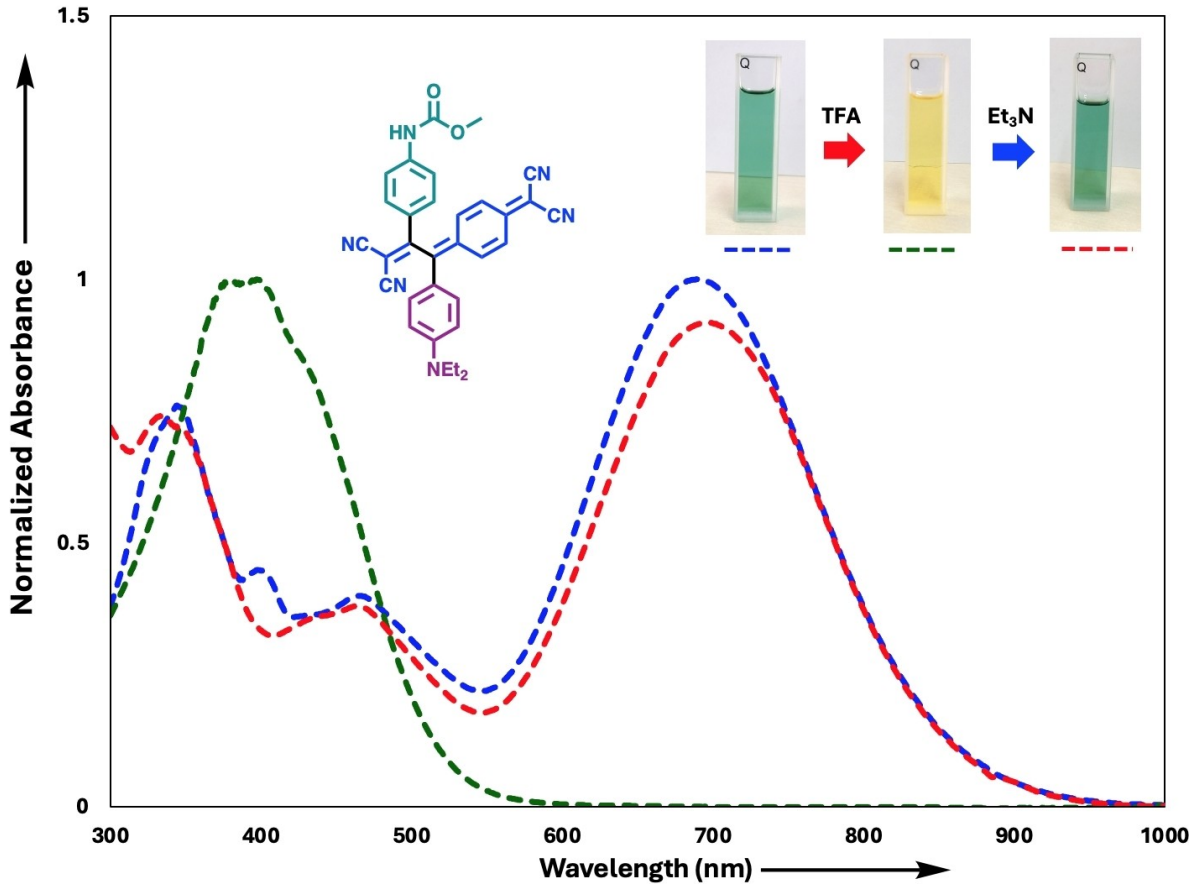

Figure 4. Protonation and neutralization experiments of chromophore **26a**.

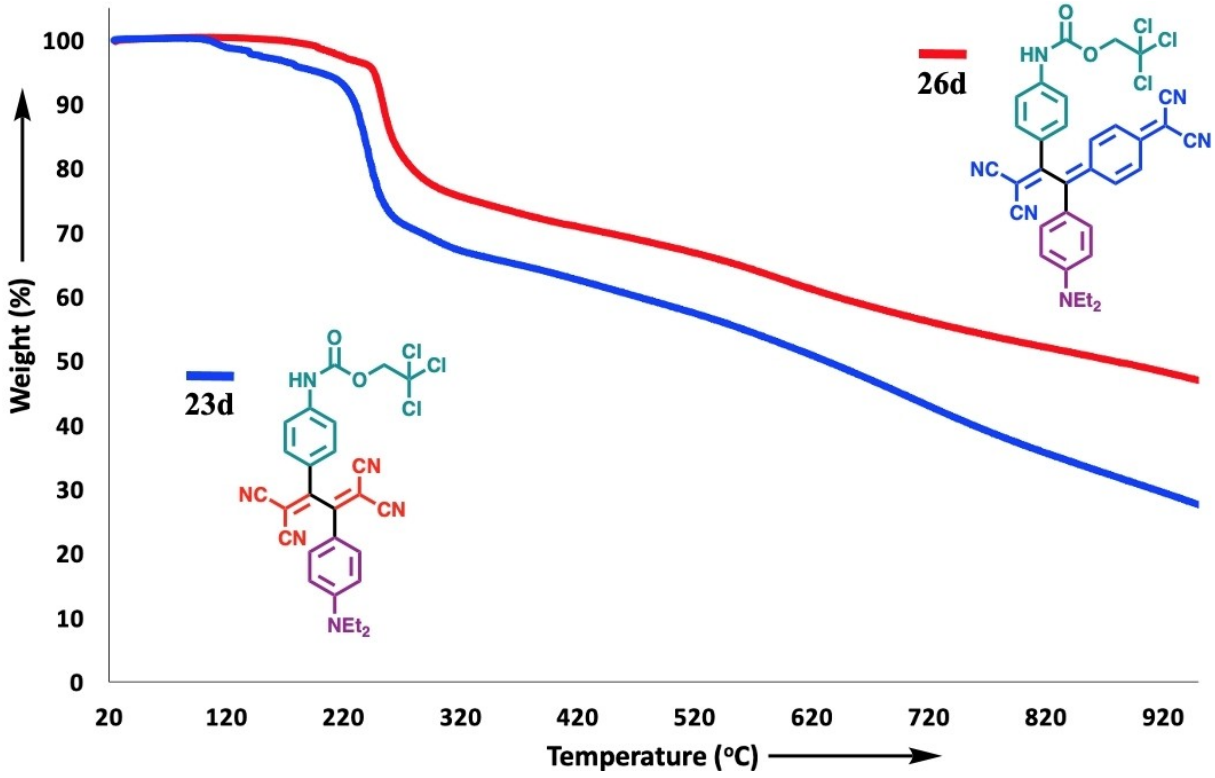

Figure 5. TGA curves for **23d** and **26d**.

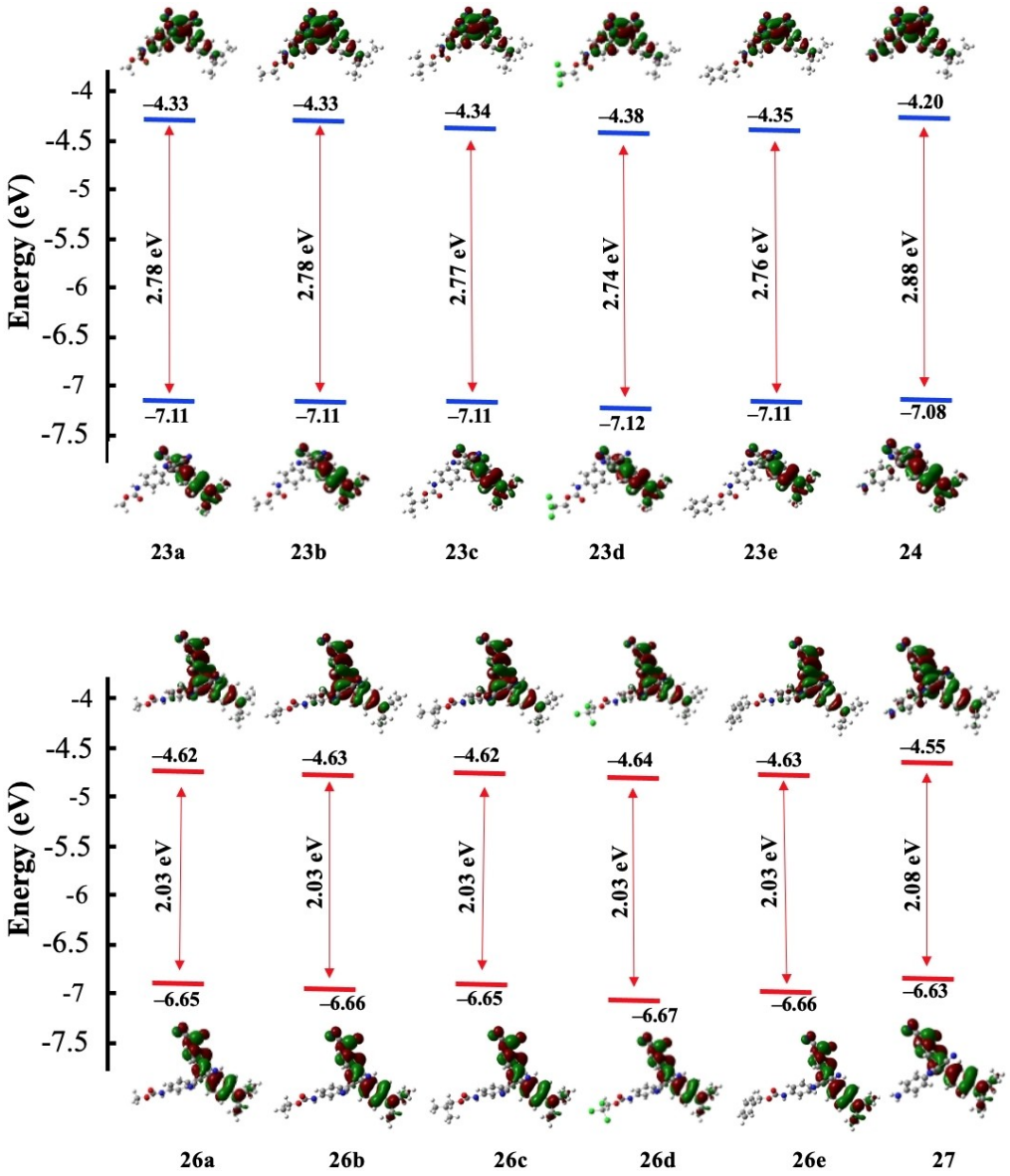

Figure 6. Frontier orbital energy level diagram of **23a–e**, **24**, **26a–e**, and **27**. The HOMO energy is derived from the optimized ground-state energy, while the LUMO energy is obtained through the calculation of the vertical excitation energy for the lowest singlet excited state.

properties (Table 1). Chromophores **23c** and **26c** were selected as representative examples. In both chromophores **23c** and **26c**, the HOMO is primarily localized on the electron-rich dialkylaniline group, while the LUMO is mainly concentrated on the electron-deficient tetracyanobutadiene (TCBD) and dicyanoquinodimethane (DCNQ) groups. The clear separation between HOMO and LUMO indicates a significant CT within the molecules. Similarly, ESP maps provide a visualization of the charge distribution within a molecule, highlighting the electron-rich and electron-poor regions. These maps indicate the areas where charge transfer is likely to occur. Thus, electron transfer is observed from the electron-rich carbamate units and dialkylamine-substituted benzenes (depicted in blue) to the electron-poor TCBD and DCNQ sites (depicted in red).

In addition to experimental TGA data, various parameters, including the electric dipole moment (μ), HOMO-LUMO gap (ΔE^{direct} and ΔE^{TD}), electronegativity (χ), global chemical hardness (η), and softness (σ), were calculated using equations 1–4 to gain deeper insights into the stability of the synthesized chromophores (Table 2).

$$\mu = [(\mu_x)^2 + (\mu_y)^2 + (\mu_z)^2]^{1/2} \quad (1)$$

$$\chi = -1/2\ (E_{HOMO} + E_{LUMO}) \quad (2)$$

$$\eta = -1/2\ (E_{HOMO} - E_{LUMO}) \quad (3)$$

$$\sigma = 1/\eta \quad (4)$$

Table 1. HOMO and LUMO visualizations, along with electrostatic potential maps ranging from −0.03 a.u. (red) to 0.03 a.u. (blue), calculated using DFT (CAM–B3LYP/6-31G++(d,p)) for the chromophores **23c** and **26c**.

	Molecular Structure	*HOMO*	*LUMO*	*ESP*
23c	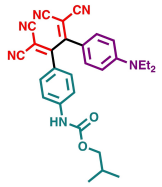	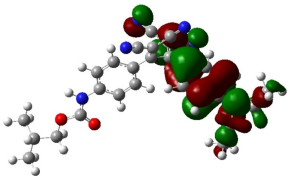	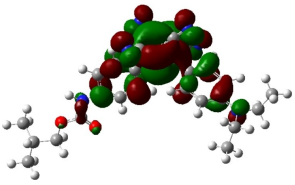	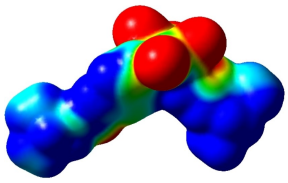
26c	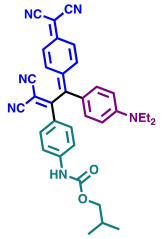	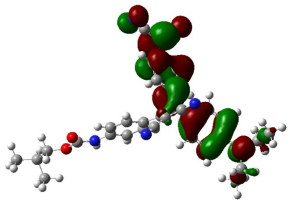	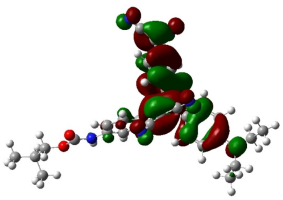	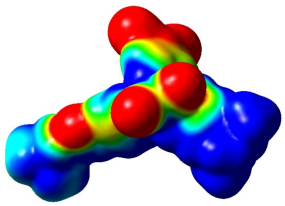

Table 2. Chemical reactivity parameters including electric dipole moment (μ), HOMO-LUMO gap (ΔE & ΔE^{TD}), electronegativity (χ), global chemical hardness (η), and softness (σ), calculated using the CAM–B3LYP/6-31G++(d,p) method in CH_2Cl_2 solvent (CPCM model).

	μ (D)	E_{HOMO} (eV)	E_{LUMO} (eV)	ΔE^{direct} (eV)	ΔE^{TD} (eV)	χ (eV)	η (eV)	σ (eV^{-})
23a	13.9047	−7.11	−2.26	4.85	2.78	4.69	2.43	0.41
23b	14.1656	−7.11	−2.25	4.86	2.78	4.68	2.43	0.41
23c	13.9462	−7.11	−2.26	4.85	2.77	4.69	2.43	0.41
24d	13.9999	−7.12	−2.30	4.82	2.74	4.71	2.41	0.42
23e	13.5377	−7.11	−2.27	4.84	2.76	4.69	2.42	0.41
24	16.7647	−7.08	−2.09	4.99	2.88	4.59	2.50	0.40
26a	22.4493	−6.65	−2.81	3.84	2.03	4.73	1.92	0.52
26b	22.6491	−6.66	−2.80	3.86	2.03	4.73	1.93	0.52
26c	22.7464	−6.65	−2.80	3.85	2.03	4.73	1.93	0.52
26d	21.9083	−6.67	−2.82	3.85	2.03	4.75	1.93	0.52
26e	22.5812	−6.66	−2.81	3.85	2.03	4.74	1.93	0.52
27	21.9871	−6.63	−2.71	3.92	2.08	4.67	1.96	0.51

Although the static dipole moment of a molecule does not directly determine its stability, molecules with high dipole moments, assuming that they have polar bonds, are more likely to undergo nucleophilic attacks in reactive environments. A comparison of the static dipole moment values calculated using Equation 1 reveals that the values for the chromophore structures obtained with TCNQ (21.9083–22.7464 D) are notably higher than those obtained with TCNE (13.5377–16.7647 D). Following our preliminary assessment of dipole moments, we concentrated on the parameters of electronegativity, global hardness, and softness to obtain a more comprehensive understanding of molecular stability using equations 2–4. There was no notable difference observed between the two groups of compounds when comparing their computed electronegativity values (4.59–4.71 for **23a–e**, **24**; 4.67–4.75 for **26a–e**, **27**). The stability of the synthesized chromophores becomes more evident when their global hardness (η) and softness (σ) values are compared. Chemical hardness (η), closely associated with the stability of a molecular system, is defined as the measure of resistance to alterations in the system's electron count.[69] A high value of η indicates a significant energy gap between the frontier orbitals of the molecule. An increase in the HOMO-LUMO energy gap corresponds to greater molecular stability. As anticipated, the group of compounds with a higher HOMO-LUMO energy gap **23a–e**, **24** exhibits greater η values (2.41–2.50 eV) compared to **26a–e**, **27** (1.92–1.96 eV). The trend in softness values, where higher values indicate greater reactivity, is the exact opposite of the trend observed in hardness values (0.40–0.42 for **23a–e**, **24**; 0.51–0.52 for **26a–e**, **27**).

NLO Studies

Unsymmetrical π-conjugated systems incorporating donor and acceptor groups, which facilitate polarization along a specific direction within the molecule, are highly favored in NLOphore design.[70] The urethane-substituted chromophores synthesized in this study, featuring donor-π-acceptor (D-π-A) structures, show potential as NLOphore candidates. To gain deeper insights into the optical properties of these compounds, average polarizability $\alpha_{(tot)}$, and first hyperpolarizability $\beta_{(tot)}$, values were calculated using equations 5 and 6. High values of $\alpha_{(tot)}$ and $\beta_{(tot)}$ are essential for achieving strong NLO properties. Generally, polarizability and hyperpolarizability tend to increase as the energy gap between frontier orbitals decreases.[71,72] Consistent with this trend, an analysis of the two groups of compounds **23a–e**, **24** and **26a–e**, **27** synthesized in this study reveals that the calculated polarizability and hyperpolarizability values are significantly higher for **26a–e**, **27** ($\alpha =$ 118.655–135.823 10^{-24} esu; $\beta =$ 292.471–318.253 10^{-30} esu) compared to those with **23a–e**, **24** ($\alpha =$ 74.674–91.326 10^{-24} esu; $\beta =$ 140.536–142.501 10^{-30} esu) (Table 3).

$$\alpha = 1/3\ (\alpha_{xx} + \alpha_{yy} + \alpha_{zz}) \tag{5}$$

$$\beta = [(\beta_{xxx} + \beta_{xyy} + \beta_{xzz})^2 + (\beta_{yyy} + \beta_{xxy} + \beta_{yzz})^2 + (\beta_{zzz} + \beta_{xxz} + \beta_{yyz})^2]^{1/2} \tag{6}$$

Encouraged by the promising results from the theoretical calculations, we directed our attention to experimentally investigating the NLO properties of the synthesized compounds. The NLO properties of **23a–e**, **24** and **26a–e**, **27** were assessed through the electric field-induced second harmonic generation (EFISHG) method (Table 3). This technique provides the scalar $\mu\beta$ product.[73] The $\mu\beta$ values are shown in Table 3.

Chromophore solutions were prepared at concentrations ranging from 10^{-2} to 10^{-3} M in $CHCl_3$. The experiments were carried out with a Raman-shifted Nd:YAG laser operating at $\lambda =$ 1907 nm. Taking into account the ±10% margin of error in the $\mu\beta$ product values measured using EFISHG, comparisons between the compound groups derived from TCNE (**23a–e**, **24**) and TCNQ (**26a–e**, **27**) should be approached with caution. In both groups, compounds **24** and **27** exhibited the lowest $\mu\beta$ values ($\mu\beta = 470\times10^{-48}$ esu for **24**; 3700×10^{-48} esu for **27**), consistent with the calculated frontier orbital energy gaps ($\Delta E^{TD} =$ 2.88 eV for **24**, 2.08 eV for **27**) for structures lacking the urethane moiety. These measurements are highly significant in demonstrating the impact of the urethane groups in the structure on the NLO properties of the compounds. A significant difference in $\mu\beta$ values is observed when comparing the two groups. The second group **26a–e**, **27**, with a lower frontier energy gaps ($\Delta E^{TD} =$ 2.03–2.08 eV), demonstrates $\mu\beta$ values ($\mu\beta = 3700\times10^{-48}-5400\times10^{-48}$ esu for **26a–e**, **27**) nearly nine times higher than those of the first group ($\mu\beta = 470\times10^{-48}-670\times10^{-48}$ esu for **23a–e**, **24**). A comparison with the literature benchmark, Disperse Red 1 ($\mu\beta = 500\times10^{-48}$)[41], based on EFISHG studies, shows that the $\mu\beta$ values of the synthesized compounds are similar to those of Disperse Red 1 in the first group **23a–e**, **24** and substantially higher in the second group **26a–e**, **27**. Comparisons with experimental EFISHG measurements of recently synthesized D–A type compounds in the literature show that the experimental $\mu\beta$ values of compounds **26a–e**, **27** specifically, are considerably higher than those of similar structures (see Figure S264 in the SI).[41,74–85] These results indicate that the synthesized urethane-containing NLOphores have high potential for NLO applications.

Conclusions

In this study, urethane-substituted alkyne substrates were developed for use in [2 + 2] cycloaddition-retroelectrocyclization reactions. It was shown that urethanes effectively activate

Table 3. Calculated and measured $\mu\beta$ values of chromophores **23a–e**, **24** and **26a–e**, **27**.

Compound	μ^a (Debye)	α^a (×10^{-24} esu)	β^a (10^{-30} esu)	$\mu\beta$ (10^{-48} esu^2·cm)[b]	$\mu\beta$ (10^{-48} esu)[c]
23a	13.1953	78.508	141.297	1865	600
23b	13.4077	80.794	141.707	1900	650
23c	13.2051	85.186	141.460	1868	510
23d	12.7346	87.017	140.536	1790	660
23e	12.8563	91.326	140.689	1809	670
24	15.5451	74.674	142.501	2215	470
26a	20.1754	123.402	306.135	6176	5200
26b	20.5924	125.464	309.012	6363	4650
26c	20.6362	130.027	303.697	6267	5400
26d	19.7785	131.798	318.253	6295	5200
26e	20.5795	135.823	314.559	6474	5000
27	19.8046	118.655	292.471	5792	3700

[a]Calculated at the DFT CAM–B3LYP/6-31G++(d,p) level in $CHCl_3$. [b]1D = 1×10^{-18} esu·cm. [c] $\mu\beta$ (2ω) at 1907 nm in $CHCl_3$, molecular concentrations used for the measurements were in the range of 10^{-3} to 10^{-2} M, $\mu\beta$ ±10%.

these reactions in the presence of $LiClO_4$. Considering the restricted substrate scope of these reactions, this work makes a significant contribution to the field. Using Sonogashira cross-coupling reactions, five alkynes groups with diverse side groups (neutral, donor, and acceptor) were synthesized. Additionally, a variety of alkyl and aryl chloroformate derivatives were utilized in urethane synthesis to enhance substituent diversity. Carbon-rich, push-pull chromophores were successfully synthesized by reacting these alkynes with the electron-deficient alkenes TCNE and TCNQ. The charge transfer absorption bands of the synthesized chromophores cover a range from the visible to the near-IR region (from 363 to 692 nm). The analysis of these absorption bands was also carried out using TD-DFT calculations. The stability characteristics of the synthesized chromophore structures were investigated through both experimental and theoretical approaches. The thermal stability analysis through TGA demonstrates that a represantative compound **26 d** exhibits significantly higher thermal stability than compound **23 d**, highlighting the influence of electron-withdrawing groups and molar mass on the stability of synthesized NLOphores. Parameters such as electronegativity, global hardness, and softness, calculated through DFT studies and consistent with frontier orbital energies, suggest that compounds **26 a–e** and **27**, obtained with TCNQ, are less stable than compounds **23 a–e** and **24**, synthesized with TCNE. In addition to their linear optical properties, urethane-substituted chromophores have demonstrated significant nonlinear optical properties in both experimental and theoretical studies. While the $\mu\beta$ values obtained from computational chemistry (1790×10^{-48} to 6474×10^{-48} esu) differ from those measured by the EFISHG technique (470×10^{-48} to 5400×10^{-48} esu), the overall trend remains consistent.

Experimental Section

General

Reagents were purchased as reagent grade and used without further purification. Commercially available chemicals were purchased by Merck, Fluka, Across, Abcr and Sigma Aldrich. Solvents for extraction or Flash column chromatography (CC) were distilled. Reactions on exclusion of air and moisture were performed in oven-dried glassware and under N_2 atmosphere. Analytical thin layer chromatography (TLC) was performed on aluminum sheets coated with 0.2 mm silica gel 60 F254 (Merck) and visualized with a UV lamp (254 or 366 nm). Evaporation in vacuo was performed at 25–60 °C and 900–10 mbar. Reported yields refer to spectroscopically and chromatographically pure compounds that were dried under high vacuum (0.1–0.05 mbar) before analytical characterization. Nuclear magnetic resonance (NMR) spectra were recorded on Bruker Avance III Ultrashield 400 Hz NMR spectrometer in $CDCl_3$. Chemical shifts δ are reported in ppm downfield from tetramethylsilane (TMS) using the residual solvent signals as an internal reference ($CDCl_3$: $\delta_H = 7.26$ ppm, $\delta_C = 77.16$ ppm). For ^1H NMR, coupling constants J are reported in Hz and the resonance multiplicity is defined as s (singlet), d (doublet), t (triplet), q (quartet), quint (quintet), sext (sextet), sept (septet), m (multiplet), and br. (broad). All spectra were recorded at 298 K. NMR spectra were processed by using MestReNova program. Infrared (IR) spectra were recorded on Thermo Scientific Nicolet iS10 ATR-IR spectrometer. Signal locations are reported as wavenumbers (cm^{-1}). The IR band intensities described as s (strong), m (medium), w (weak), br. (broad). High-resolution mass spectrometry (HR-MS) was performed by the MS-service of METU Central Laboratory, Turkey. Spectra were processed in electrospray ionization with positive or negative modes using Time of Flight mass analyzer. Masses are reported in m/z units as the molecule ion as $[M + H]^+$, $[M]^+$ or $[M-H]^-$.

General procedure for the synthesis of 8 a–e. Compound **6** (2.00 g, 9.13 mmol, 1.00 equiv.) was dissolved in 10 mL of THF, cooled in an ice bath, and treated with pyridine (1.30 equiv.). Subsequently, the appropriate chloroformates **7 a–e** (1.20 equiv.) were added. The reaction mixture was gradually warmed to room temperature and stirred for one hour. After confirming the reaction's completion, it was quenched with water, extracted with CH_2Cl_2 (3×30 mL), dried over $MgSO_4$, and concentrated under reduced pressure. The resulting solid was purified by column chromatography (CC), yielding products **8 a–e** with yields ranging from 78% to 99%.[86]

Compound 8 a: yield: 2.27 g (90%); white solid; $R_f = 0.68$ (SiO_2; 1:1 hexanes/ethyl acetate); ^1H NMR (400 MHz, $CDCl_3$, 298 K); $\delta = 7.60$ (quasi d, $J = 8.4$ Hz, 2H), 7.17 (quasi d, $J = 8.4$ Hz, 2H), 6.58 (br. s, 1H), 3.77 ppm (s, 3H); $^{13}C\{^1H\}$ NMR (100 MHz, $CDCl_3$, 298 K); $\delta = 154.0$, 138.0, 137.8, 120.7, 86.5, 52.6 ppm. Spectral data is consistent with the literature.[87]

Compound 8 b: yield: 2.64 g (99%); white solid; $R_f = 0.65$ (SiO_2; CH_2Cl_2); m.p. = 106–108 °C; ^1H NMR (400 MHz, $CDCl_3$, 298 K); $\delta = {}^1H$ NMR (400 MHz, $CDCl_3$, 298 K) $\delta = 7.59$ (quasi d, $J = 8.4$ Hz, 2H), 7.17 (quasi d, $J = 8.4$ Hz, 2H), 6.58 (br. s, 1H), 4.22 (q, $J = 7.1$ Hz, 2H), 1.30 ppm (t, $J = 7.1$ Hz, 3H); $^{13}C\{^1H\}$ NMR (100 MHz, $CDCl_3$, 298 K); $\delta = 153.5$, 138.0, 137.9, 120.6, 86.3, 61.5, 14.6 ppm; IR (ATR): $\tilde{\nu} = 3284$ (m), 1696 (s) cm^{-1}; HRMS (ESI-TOF) m/z: $[M-H]^-$ Calcd. for $C_9H_9NO_2I^-$ 289.9678; Found 289.9679.

Compound 8 c: yield: 2.27 g (78%); white solid; $R_f = 0.72$ (SiO_2; 1:1 hexanes/ethyl acetate); m.p. = 115–117 °C; ^1H NMR (400 MHz, $CDCl_3$, 298 K); $\delta = 7.59$ (quasi d, $J = 8.8$ Hz, 2H), 7.17 (quasi d, $J = 8.8$ Hz, 2H), 6.60 (br. s, 1H), 3.94 (d, $J = 6.7$ Hz, 2H), 2.02–1.90 (m, 1H), 0.96 ppm (d, $J = 6.7$ Hz, 6H); $^{13}C\{^1H\}$ NMR (100 MHz, $CDCl_3$, 298 K); $\delta = 153.6$, 138.03, 137.95, 120.6, 86.3, 71.7, 28.1, 19.2 ppm; IR (ATR): $\tilde{\nu} = 3327$ (m), 1694 (s) cm^{-1}; HRMS (ESI-TOF) m/z: $[M-H]^-$ Calcd. for $C_{11}H_{13}NO_2I^-$ 317.9991; Found 317.9990.

Compound 8 d: yield: 3.27 g (91%); light yellow solid; $R_f = 0.79$ (SiO_2; 2:1 hexanes/ethyl acetate); ^1H NMR (400 MHz, $CDCl_3$, 298 K); $\delta = 7.63$ (quasi d, $J = 8.5$ Hz, 2H), 7.20 (quasi d, $J = 8.5$ Hz, 2H), 6.89 (br. s, 1H), 4.82 ppm (s, 2H); $^{13}C\{^1H\}$ NMR (100 MHz, $CDCl_3$, 298 K); $\delta = 151.5$, 138.1, 136.9, 120.9, 95.2, 87.5, 74.7 ppm. Spectral data is consistent with the literature.[88]

Compound 8 e: yield: 2.58 g (80%); white solid; $R_f = 0.55$ (SiO_2; 1:1 hexanes/ethyl acetate); ^1H NMR (400 MHz, $CDCl_3$, 298 K); $\delta = 7.60$ (quasi d, $J = 8.8$ Hz, 2H), 7.41–7.34 (m, 5H), 7.17 (quasi d, $J = 8.8$ Hz, 2H), 6.64 (br. s, 1H), 5.19 ppm (s, 2H); $^{13}C\{^1H\}$ NMR (100 MHz, $CDCl_3$, 298 K); $\delta = 153.2$, 138.0, 137.7, 135.9, 128.8, 128.6, 128.5, 120.6, 86.5, 67.3 ppm. Spectral data is consistent with the literature.[89]

General procedure for the synthesis of 10 a–e. Compounds **8 a–e** (1.00 equiv.) were dissolved in 10 mL of triethylamine in a flask sealed with a rubber septum, and the atmosphere was purged with N_2 for 10 minutes. Subsequently, CuI (0.03 equiv.) and $[Pd(PPh_3)_2Cl_2]$ (0.03 equiv.) were added to the flask, followed by an additional 10-minute N_2 purge. TMSA **9** (1.10 equiv.) was then introduced via syringe, and the reaction mixture was stirred at room temperature overnight. Upon completion, the solvent was removed under reduced pressure, and the resulting solid was extracted twice with CH_2Cl_2 (50 mL×2). The combined organic layers were dried over

$MgSO_4$, filtered, and concentrated. Purification by CC (SiO_2; 2:1 hexanes/ethyl acetate) yielded products **10a–e** in 61–95% yields.[90]

Compound 10a: (Starting material **8a**: 1.99 g, 7.18 mmol); yield: 1.09 g (61%); yellow solid; R_f = 0.82 (SiO_2; 1:1 hexanes/ethyl acetate); m.p. = 128–130 °C; ^{1}H NMR (400 MHz, $CDCl_3$, 298 K); δ = 7.41 (quasi d, J = 8.7 Hz, 2H), 7.32 (quasi d, J = 8.7 Hz, 2H), 6.65 (br. s, 1H), 3.77 (s, 3H), 0.24 ppm (s, 9H); ^{13}C{^{1}H} NMR (100 MHz, $CDCl_3$, 298 K); δ = 153.9, 138.2, 133.0, 118.2, 118.0, 105.0, 93.5, 52.6, 0.1 ppm; IR (ATR): $\tilde{\nu}$ = 3279 (m), 2956 (m), 2159 (s), 1702 (s) cm^{-1}; HRMS (ESI-TOF) m/z: $[M-H]^-$ Calcd. for $C_{13}H_{16}NO_2Si^-$ 246.0950; Found 246.0944.

Compound 10b: (Starting material **8b**: 2.52 g, 8.66 mmol); yield: 2.14 g (95%); yellow solid; R_f = 0.48 (SiO_2; 5:1 hexanes/ethyl acetate); m.p. = 112–114 °C; ^{1}H NMR (400 MHz, $CDCl_3$, 298 K); δ = 7.40 (quasi d, J = 8.7 Hz, 2H), 7.32 (quasi d, J = 8.7 Hz, 2H), 6.64 (br. s, 1H), 4.22 (q, J = 7.1 Hz, 2H), 1.31 (t, J = 7.1 Hz, 3H), 0.24 ppm (s, 9H); ^{13}C{^{1}H} NMR (100 MHz, $CDCl_3$, 298 K); δ = 153.4, 138.3, 133.0, 118.1, 117.9, 105.0, 93.5, 61.5, 14.7, 0.1 ppm; IR (ATR): $\tilde{\nu}$ = 3321 (m), 2961 (w), 2157 (s), 1704 (s) cm^{-1}; HRMS (ESI-TOF) m/z: $[M-H]^-$ Calcd. for $C_{14}H_{18}NO_2Si^-$ 260.1107; Found 260.1102.

Compound 10c: (Starting material **8c**: 2.01 g, 6.30 mmol); yield: 1.43 g (78%); yellow solid; R_f = 0.72 (SiO_2; 3:1 hexanes/ethyl acetate); m.p. = 130–132 °C; ^{1}H NMR (400 MHz, $CDCl_3$, 298 K); δ = 7.40 (quasi d, J = 8.3 Hz, 2H), 7.33 (quasi d, J = 8.3 Hz, 2H), 6.74 (br. s, 1H), 3.94 (d, J = 6.7 Hz, 2H), 1.90–2.02 (m, 1H), 0.95 (d, J = 6.7 Hz, 6H), 0.24 ppm (s, 9H); ^{13}C{^{1}H} NMR (100 MHz, $CDCl_3$, 298 K); δ = 153.5, 138.3, 138.1, 133.1, 118.1, 105.0, 93.5, 71.7, 28.1, 19.2, 0.2 ppm; IR (ATR): $\tilde{\nu}$ = 3318 (m), 2959 (m), 2153 (w), 1698 (s) cm^{-1}; HRMS (ESI-TOF) m/z: $[M-H]^-$ Calcd. for $C_{16}H_{22}NO_2Si^-$ 288.1420; Found 288.1423.

Compound 10d: (Starting material **8d**: 2.79 g, 7.07 mmol); yield: 2.16 g (84%); yellow solid; R_f = 0.48 (SiO_2; 5:1 hexanes/ethyl acetate); m.p. = 130–132 °C; ^{1}H NMR (400 MHz, $CDCl_3$, 298 K); δ = 7.44 (quasi d, J = 8.6 Hz, 2H), 7.36 (quasi d, J = 8.6 Hz, 2H), 6.92 (br. s, 1H), 4.82 (s, 2H), 0.24 ppm (s, 9H); ^{13}C{^{1}H} NMR (100 MHz, $CDCl_3$, 298 K); δ = 151.4, 137.3, 133.1, 118.8, 118.4, 104.7, 95.2, 94.0, 74.6, 0.1 ppm; IR (ATR): $\tilde{\nu}$ = 3304 (m), 2959 (w), 2156 (m), 1714 (s) cm^{-1}; HRMS (ESI-TOF) m/z: $[M-H]^-$ Calcd. for $C_{14}H_{15}Cl_3NO_2Si^-$ 361.9938; Found 361.9932.

Compound 10e: (Starting material **8d**: 2.44 g, 7.19 mmol); yield: 2.09 g (94%); yellow solid; R_f = 0.52 (SiO_2; 5:1 hexanes/ethyl acetate); ^{1}H NMR (400 MHz, $CDCl_3$, 298 K); δ = 7.43–7.31 (m, 9H), 6.73 (br. s, 1H), 5.20 (s, 2H), 0.24 ppm (s, 9H); ^{13}C{^{1}H} NMR (100 MHz, $CDCl_3$, 298 K); δ = 153.2, 138.1, 135.9, 133.0, 128.7, 128.5, 128.4, 118.2, 118.0, 105.0, 93.6, 67.3, 0.1 ppm. Spectral data is consistent with the literature.[90]

General procedure for the synthesis of 1a–e. A solution of **10a–e** (1.00 equiv.) in tetrahydrofuran (THF) was cooled to 0 °C using an ice bath. Subsequently, tetrabutylammonium fluoride (TBAF, 1.0 M, 1.20 equiv.) was added, and the reaction mixture was stirred for 15 minutes. After completion, the reaction was quenched with saturated $NaHCO_3$, followed by extraction with ethyl acetate (2×50 mL). The organic layers were dried over $MgSO_4$, filtered, and concentrated. Purification by CC provided products **1a–e** in yields ranging from 30% to 83%.

Compound 1a: (Starting material **10a**: 1.05 g, 4.24 mmol); yield: 589 mg (79%); yellow solid; R_f = 0.84 (SiO_2; 1:1 hexanes/ethyl acetate); ^{1}H NMR (400 MHz, $CDCl_3$, 298 K); δ = 7.44 (quasi d, J = 8.3 Hz, 2H), 7.35 (quasi d, J = 8.3 Hz, 2H), 6.63 (br. s, 1H), 3.81 (s, 3H), 3.03 ppm (s, 1H); ^{13}C{^{1}H} NMR (100 MHz, $CDCl_3$, 298 K); δ = 153.8, 138.5, 133.2, 118.3, 117.0, 83.5, 76.7, 52.7 ppm. Spectral data is consistent with the literature.[91]

Compound 1b: (Starting material **10b**: 2.14 g, 8.19 mmol); yield: 1.28 g (83%); yellow solid; R_f = 0.57 (SiO_2; 5:1 hexanes/ethyl acetate); ^{1}H NMR (400 MHz, DMSO-d_6, 298 K); δ = 9.87 (br. s, 1H), 7.47 (quasi d, J = 8.6 Hz, 2H), 7.38 (quasi d, J = 8.6 Hz, 2H), 4.12 (q, J = 7.1 Hz, 2H), 4.07 (s, 1H), 1.23 ppm (t, J = 7.1 Hz, 3H); ^{13}C{^{1}H} NMR (100 MHz, DMSO-d_6, 298 K); δ = 153.5, 140.0, 132.5, 118.0, 115.3, 83.7, 79.7, 60.5, 14.6 ppm. Spectral data is consistent with the literature.[92]

Compound 1c: (Starting material **10c**: 1.30 g, 4.49 mmol); yield: 789 mg (81%); yellow solid; R_f = 0.88 (SiO_2; CH_2Cl_2); m.p. = 81–83 °C; ^{1}H NMR (400 MHz, $CDCl_3$, 298 K); δ = 7.43 (quasi d, J = 8.4 Hz, 2H), 7.35 (quasi d, J = 8.4 Hz, 2H), 6.71 (br, s, 1H), 3.95 (d, J = 6.6 Hz, 2H), 3.03 (s, 1H), 2.03–1.91 (m, 1H), 0.96 ppm (d, J = 6.6 Hz, 6H); ^{13}C{^{1}H} NMR (100 MHz, $CDCl_3$, 298 K); δ = 153.5, 138.7, 133.2, 118.3, 116.9, 83.6, 76.6, 71.7, 28.1, 19.2 ppm; IR (ATR): $\tilde{\nu}$ = 3338 (m), 3299 (m), 2107 (w), 1702 (s) cm^{-1}; HRMS (ESI-TOF) m/z: $[M-H]^-$ Calcd. for $C_{13}H_{14}NO_2^-$ 216.1025; Found 216.1016.

Compound 1d: (Starting material **10d**: 2.00 g, 5.48 mmol); yield: 485 mg (30%); yellow solid; R_f = 0.79 (SiO_2; 1:1 CH_2Cl_2); m.p. = 113–115 °C; ^{1}H NMR (400 MHz, $CDCl_3$, 298 K); δ = 7.44 (quasi d, J = 8.4 Hz, 2H), 7.35 (quasi d, J = 8.4 Hz, 2H), 6.66 (br. s, 1H), 3.78 (s, 2H), 3.03 ppm (s, 1H); ^{13}C{^{1}H} NMR (100 MHz, $CDCl_3$, 298 K); δ = 151.7, 139.1, 132.6, 118.4, 116.1, 95.8, 83.5, 80.0, 73.5 ppm; IR (ATR): $\tilde{\nu}$ = 3306 (m), 3270 (m), 2101 (w), 1714 (s) cm^{-1}; HRMS (ESI-TOF) m/z: $[M-H]^-$ Calcd. for $C_{11}H_7Cl_3NO_2^-$ 289.9542; Found 289.9540.

Compound 1e: (Starting material **10e**: 1.91 g, 5.90 mmol); yield: 903 mg (61%); yellow solid; R_f = 0.50 (SiO_2; 5:1 hexanes/ethyl acetate); ^{1}H NMR (400 MHz, $CDCl_3$, 298 K); δ = 7.34–7.46 (m, 9H), 6.73 (s, 1H), 5.20 (s, 2H), 3.03 ppm (s, 1H); ^{13}C{^{1}H} NMR (100 MHz, $CDCl_3$, 298 K); δ = 153.1, 138.4, 135.9, 133.2, 128.8, 128.6, 128.5, 118.2, 117.0, 83.5, 76.7, 67.4 ppm. Spectral data is consistent with the literature.[93]

General procedure for the synthesis of 12a–e. Under an inert nitrogen atmosphere, TCNE **11** (2.07 equiv.) was added to a solution of compound **1a–e** (1.00 equiv.) in CH_2Cl_2 (3 mL). The reaction mixture was stirred overnight at room temperature, and the resulting product was recrystallized from chloroform to yield pure red-colored chromophores **12a–e** in between 36–82% yield.

Compound 12a: (Starting material **1a**: 50 mg, 0.29 mmol); yield: 43 mg (50%); red solid; R_f = 0.73 (SiO_2; 2:3 hexanes/ethyl acetate); m.p. = 209–211 °C; ^{1}H NMR (400 MHz, $CDCl_3$, 298 K); δ = 8.02 (s, 1H), 7.67 (quasi d, J = 8.8 Hz, 2H), 7.44 (quasi d, J = 8.8 Hz, 2H), 6.94 (br. s, 1H), 3.82 ppm (s, 3H); ^{13}C{^{1}H} NMR (100 MHz, $CDCl_3$, 298 K); δ = 161.4, 153.2, 152.9, 143.8, 130.9, 124.4, 119.0, 111.74, 111.65, 111.2, 108.6, 98.3, 90.3, 53.1 ppm; UV/vis (CH_2Cl_2): λ_{max} (ε) = 290 (2.93×10^4), 447 nm (6.55×10^3 M^{-1} cm^{-1}); IR (ATR): $\tilde{\nu}$ = 3345 (s), 2224 (m), 1721 (s) cm^{-1}; HRMS (ESI-TOF) m/z: $[M-H]^-$ Calcd. for $C_{16}H_8N_5O_2^-$ 302.0678; Found 302.0670.

Compound 12b: (Starting material **1b**: 50 mg, 0.26 mmol); yield: 56 mg (67%); red solid; R_f = 0.57 (SiO_2; 2:3 hexanes/ethyl acetate); m.p. = 128–130 °C; ^{1}H NMR (400 MHz, $CDCl_3$, 298 K); δ = 8.02 (s, 1H), 7.66 (quasi d, J = 8.7 Hz, 2H), 7.43 (quasi d, J = 8.7 Hz, 2H), 6.94 (br. s, 1H), 4.27 (q, J = 7.1 Hz, 2H), 1.33 ppm (t, J = 7.1 Hz, 3H); ^{13}C{^{1}H} NMR (100 MHz, $CDCl_3$, 298 K); δ = 161.4, 153.1, 152.9, 144.0, 130.9, 124.3, 119.0, 111.74, 111.70, 111.2, 108.6, 98.3, 90.1, 62.2, 14.6 ppm; UV/vis (CH_2Cl_2): λ_{max} (ε) = 290 (3.01×10^4), 447 nm (7.10×10^3 M^{-1} cm^{-1}); IR (ATR): $\tilde{\nu}$ = 3293 (m), 2233 (m), 1705 (s) cm^{-1}; HRMS (ESI-TOF) m/z: $[M-H]^-$ Calcd. for $C_{17}H_{10}N_5O_2^-$ 316.0834; Found 316.0837.

Compound 12c: (Starting material **1c**: 50 mg, 0.23 mmol); yield: 40 mg (50%); red solid; R_f = 0.76 (SiO_2; 2:3 hexanes/ethyl acetate); m.p. = 121–123 °C; ^{1}H NMR (400 MHz, $CDCl_3$, 298 K); δ = 8.02 (s, 1H), 7.68 (quasi d, J = 8.6 Hz, 2H), 7.44 (quasi d, J = 8.6 Hz, 2H), 6.96 (br. s,

1H), 3.99 (d, J = 6.7 Hz, 2H), 2.03–1.95 (m, 1H), 0.98 ppm (t, J = 6.7 Hz, 6H); $^{13}C\{^1H\}$ NMR (100 MHz, $CDCl_3$, 298 K); δ = 161.4, 153.0, 152.9, 144.0, 130.9, 124.3, 119.0, 111.74, 111.69, 111.2, 108.6, 98.3, 90.1, 72.2, 28.0, 19.2 ppm; UV/vis (CH_2Cl_2): λ_{max} (ε) = 291 (3.39×10^4), 447 nm (7.80×10^3 M^{-1} cm^{-1}); IR (ATR): $\tilde{\nu}$ = 3369 (m), 2221 (m), 1738 (s) cm^{-1}; HRMS (ESI-TOF) m/z: $[M-H]^-$ Calcd. for $C_{19}H_{14}N_5O_2^-$ 344.1147; Found 344.1130.

Compound 12d: (Starting material **1d**: 50 mg, 0.17 mmol); yield: 26 mg (36%); red solid; R_f = 0.80 (SiO_2; 2:3 hexanes/ethyl acetate); m.p. = 110–112 °C; ^1H NMR (400 MHz, $CDCl_3$, 298 K); δ = 8.03 (s, 1H), 7.72 (quasi d, J = 8.6 Hz, 2H), 7.46 (quasi d, J = 8.6 Hz, 2H), 7.24 (br. s, 1H), 4.85 ppm (s, 2H); $^{13}C\{^1H\}$ NMR (100 MHz, $CDCl_3$, 298 K); δ = 161.3, 152.6, 151.0, 142.8, 130.8, 125.1, 119.5, 111.7, 111.5, 111.0, 108.6, 98.4, 94.8, 91.3, 75.0 ppm; UV/vis (CH_2Cl_2): λ_{max} (ε) = 288 (1.99×10^4), 431 nm (4.80×10^3 M^{-1} cm^{-1}); IR (ATR): $\tilde{\nu}$ = 3305 (m), 2227 (w), 1751 (s) cm^{-1}; HRMS (ESI-TOF) m/z: $[M-H]^-$ Calcd. for $C_{17}H_7Cl_3N_5O_2^-$ 417.9665; Found 417.9666.

Compound 12e: (Starting material **1e**: 50 mg, 0.20 mmol); yield: 62 mg (82%); red solid; R_f = 0.78 (SiO_2; 2:3 hexanes/ethyl acetate); m.p. = 168–170 °C; ^1H NMR (400 MHz, $CDCl_3$, 298 K); δ = 8.00 (s, 1H), 7.66 (quasi d, J = 8.5 Hz, 2H), 7.43–7.36 (m, 7H), 7.05 (br. s, 1H), 5.23 ppm (s, 2H); $^{13}C\{^1H\}$ NMR (100 MHz, $CDCl_3$, 298 K); δ = 161.4, 153.0, 152.6, 143.8, 135.4, 130.9, 128.90, 128.86, 128.6, 124.5, 119.1, 111.74, 111.67, 111.2, 108.6, 98.3, 90.3, 67.9 ppm; UV/vis (CH_2Cl_2): λ_{max} (ε) = 278 (3.48×10^4), 444 nm (6.25×10^3 M^{-1} cm^{-1}); IR (ATR): $\tilde{\nu}$ = 3373 (m), 2224 (m), 1755 (s) cm^{-1}; HRMS (ESI-TOF) m/z: $[M-H]^-$ Calcd. for $C_{22}H_{12}N_5O_2^-$ 378.0991; Found 378.0989.

Synthesis of Compound 14

4-Iodoaniline (**6**) (1.00 g, 4.57 mmol, 1.00 equiv.) was dissolved in 10 mL of diisopropylamine (DIPA) in a flask sealed with a rubber septum. The atmosphere was purged with nitrogen for 10 minutes. CuI (26 mg, 0.14 mmol, 0.03 equiv.) and $[Pd(PPh_3)_2Cl_2]$, 96 mg, 0.14 mmol, 0.03 equiv.) were then added, followed by an additional 10 minutes of nitrogen purging. Phenylacetylene (**13**) (560 mg, 5.48 mmol, 1.20 equiv.) was introduced via syringe, and the reaction mixture was stirred at room temperature overnight. Upon completion, the solvent was removed under reduced pressure, and the residue was extracted with dichloromethane (50 mL×2). The combined organic layers were dried over MgSO4, filtered, and concentrated. Purification by CC (SiO_2; CH_2Cl_2) afforded compound **14**.

Compound 14: yield: 707 mg (80%); brown solid; R_f = 0.65 (SiO_2; CH_2Cl_2); m.p. = 124–126 °C; ^1H NMR (400 MHz, $CDCl_3$, 298 K); δ = 7.50 (quasi d, J = 7.4 Hz, 2H), 7.37–7.28 (m, 5H), 6.64 (quasi d, J = 8.1 Hz, 2H), 3.82 ppm (br. s, 2H); $^{13}C\{^1H\}$ NMR (100 MHz, $CDCl_3$, 298 K); δ = 146.8, 133.1, 131.5, 128.4, 127.8, 124.0, 114.9, 112.7, 90.3, 87.4 ppm. Spectral data is consistent with the literature.[94]

General Procedure for the Synthesis of 2a–f

Compound **14** (1.00 equiv.) was dissolved in 10 mL of THF and cooled using an ice bath. Pyridine (1.30 equiv.) was then added, followed by the dropwise addition of the corresponding chloroformates **7a–f** (1.20 equiv.). The reaction mixture was gradually warmed to room temperature and stirred for one hour. Upon completion, the reaction was quenched with water, extracted with CH_2Cl_2 (3×30 mL), and the combined organic layers were dried over $MgSO_4$. The solvent was removed under reduced pressure, and the resulting solid was purified by CC to afford products **2a–f** with yields ranging from 56% to 90%.[86]

Compound 2a: (Starting material **14**: 280 mg, 1.45 mmol) yield: 310 mg (85%); yellow solid; R_f = 0.71 (SiO_2; 4:1 hexanes/ethyl acetate); m.p. = 136–138 °C; ^1H NMR (400 MHz, $CDCl_3$, 298 K); δ = 7.54–7.46 (m, 4H), 7.41–7.31 (m, 5H), 6.69 (br. s, 1H), 3.79 ppm (s, 3H); $^{13}C\{^1H\}$ NMR (100 MHz, $CDCl_3$, 298 K); δ = 153.9, 138.0, 132.5, 131.6, 128.4, 128.2, 123.4, 118.4, 118.0, 89.3, 88.9, 52.6 ppm; IR (ATR): $\tilde{\nu}$ = 3347 (m), 2215 (w), 1712 (s) cm^{-1}; HRMS (ESI-TOF) m/z: $[M-H]^-$ Calcd. for $C_{16}H_{12}NO_2^-$ 250.0868; Found 250.0868.

Compound 2b: (Starting material **14**: 280 mg, 1.45 mmol) yield: 346 mg (90%); yellow solid; R_f = 0.61 (SiO_2; 4:1 hexanes/ethyl acetate); m.p. = 110–112 °C; ^1H NMR (400 MHz, $CDCl_3$, 298 K); δ = 7.54–7.50 (m, 2H), 7.48 (quasi d, J = 8.7 Hz, 2H), 7.41–7.32 (m, 5H), 6.70 (br. s, 1H), 4.24 (q, J = 7.1 Hz, 2H), 1.32 ppm (t, J = 7.1 Hz, 3H); $^{13}C\{^1H\}$ NMR (100 MHz, $CDCl_3$, 298 K); δ = 153.5, 138.2, 132.6, 131.6, 128.5, 128.2, 123.5, 118.3, 118.0, 89.3, 88.9, 61.6, 14.7 ppm; IR (ATR): $\tilde{\nu}$ = 3266 (m), 2216 (w), 1737 (s) cm^{-1}; HRMS (ESI-TOF) m/z: $[M+H]^+$ Calcd. for $C_{17}H_{16}NO_2^+$ 266.1181; Found 266.1181.

Compound 2c: (Starting material **14**: 280 mg, 1.45 mmol) yield: 380 mg (89%); yellow solid; R_f = 0.78 (SiO_2; 9:1 hexanes/ethyl acetate); m.p. = 168–170 °C; ^1H NMR (400 MHz, $CDCl_3$, 298 K); δ = 7.54–7.47 (m, 4H), 7.43–7.32 (m, 5H), 6.88 (br. s, 1H), 3.97 (d, J = 6.5 Hz, 2H), 2.02–1.94 (m, 1H), 0.98 ppm (d, J = 6.5 Hz, 6H); $^{13}C\{^1H\}$ NMR (100 MHz, $CDCl_3$, 298 K); δ = 153.6, 138.2, 132.6, 131.6, 128.4, 128.2, 123.5, 118.4, 118.0, 89.3, 88.9, 71.7, 28.1, 19.2 ppm; IR (ATR): $\tilde{\nu}$ = 3298 (m), 2217 (w), 1700 (s) cm^{-1}; HRMS (ESI-TOF) m/z: $[M+H]^+$ Calcd. for $C_{19}H_{20}NO_2^+$ 294.1494; Found 294.1502.

Compound 2d: (Starting material **14**: 280 mg, 1.45 mmol) yield: 357 mg (67%); yellow solid; R_f = 0.53 (SiO_2; 4:1 hexanes/ethyl acetate); m.p. = 123–125 °C; ^1H NMR (400 MHz, $CDCl_3$, 298 K); δ = 7.54–7.49 (m, 4H), 7.43 (quasi d, J = 8.3 Hz, 2H), 7.38–7.32 (m, 3H), 6.92 (br. s, 1H), 4.84 ppm (s, 2H); $^{13}C\{^1H\}$ NMR (100 MHz, $CDCl_3$, 298 K); δ = 151.4, 137.1, 132.7, 131.7, 128.5, 128.4, 123.3, 119.0, 118.6, 95.2, 89.3, 89.0, 74.7 ppm; IR (ATR): $\tilde{\nu}$ = 3359 (m), 1716 (m) cm^{-1}; HRMS (ESI-TOF) m/z: $[M-H]^-$ Calcd. for $C_{17}H_{11}Cl_3NO_2^-$ 365.9855; Found 365.9855.

Compound 2e: (Starting material **14**: 280 mg, 1.45 mmol) yield: 424 mg (89%); yellow solid; R_f = 0.56 (SiO_2; 4:1 hexanes/ethyl acetate); m.p. = 147–149 °C; ^1H NMR (400 MHz, $CDCl_3$, 298 K); δ = 7.54–7.45 (m, 4H), 7.42–7.31 (m, 10H), 6.72 (br. s, 1H), 5.21 ppm (s, 2H); $^{13}C\{^1H\}$ NMR (100 MHz, $CDCl_3$, 298 K); δ = 153.2, 137.9, 136.0, 132.6, 131.7, 128.8, 128.6, 128.51, 128.47, 128.3, 123.5, 118.4, 118.3, 89.3, 89.0, 67.4 ppm; IR (ATR): $\tilde{\nu}$ = 3300 (m), 2219 (w), 1697 (s) cm^{-1}; HRMS (ESI-TOF) m/z: $[M+H]^+$ Calcd. for $C_{22}H_{18}NO_2^+$ 328.1338; Found 328.1349.

Compound 2f: (Starting material **14**: 300 mg, 1.55 mmol); yield: 314 mg (56%); white solid; R_f = 0.78 (SiO_2; 2:1 hexanes/ethyl acetate); ^1H NMR (400 MHz, $CDCl_3$, 298 K); δ = 8.29 (quasi d, J = 9.2 Hz, 2H), 7.56–7.51 (m, 4H), 7.45 (quasi d, J = 8.5 Hz, 2H), 7.40 (quasi d, J = 9.2 Hz, 2H), 7.37–7.35 (m, 3H), 7.08 ppm (br. s, 1H); $^{13}C\{^1H\}$ NMR (100 MHz, $CDCl_3$, 298 K); δ = 155.3, 150.0, 145.3, 136.7, 132.8, 131.7, 128.52, 128.46, 125.4, 123.3, 122.3, 119.5, 118.8, 89.5, 88.9 ppm; IR (ATR): $\tilde{\nu}$ = 3305 (m), 1730 (s) cm^{-1}; HRMS (ESI-TOF) m/z: $[M+H]^+$ Calcd. for $C_{21}H_{15}N_2O_4^+$ 359.1032; Found 359.1045.

General procedure for the synthesis of 15a–e and 16. Under an inert nitrogen atmosphere, TCNE (**11**) (1.5 equiv.) and $LiClO_4$ (2.00 equiv.) were added to a solution of compound **2a–f** (1.00 equiv.) in acetonitrile (2 mL). The reaction mixture was heated to reflux at 82 °C and stirred under inert conditions for 3 days. The resulting mixture was purified using CC to yield gel-like bright yellow solids **15a–e** in 50–96% yield or a red solid **16** in 8% yield.

Compound 15a: (Starting material **2a**: 40 mg, 0.16 mmol); yield: 52 mg (86%); bright yellow solid; R_f = 0.85 (SiO_2; 1:1 hexanes/ethyl

acetate); m.p. = 102–104 °C; ^{1}H NMR (400 MHz, $CDCl_3$, 298 K); δ = 7.76–7.53 (m, 9H), 7.13 (br. s, 1H), 3.82 ppm (s, 3H); $^{13}C\{^1H\}$ NMR (100 MHz, $CDCl_3$, 298 K); δ = 167.7, 165.7, 153.2, 144.5, 134.8, 131.43, 131.38, 130.2, 129.5, 125.3, 118.9, 112.3, 111.71, 111.67, 111.2, 87.9, 84.3, 53.2 ppm; UV/vis (CH_2Cl_2): λ_{max} (ε) = 299 (2.08×10^4), 330 (2.35×10^4), 382 nm (1.95×10^4 M^{-1} cm^{-1}); IR (ATR): $\tilde{\nu}$ = 3337 (m), 2228 (m), 1734 (s) cm^{-1}; HRMS (ESI-TOF) m/z: $[M-H]^-$ Calcd. for $C_{22}H_{12}N_5O_2^-$ 378.0991; Found 378.0991.

Compound 15b: (Starting material **2b**: 40 mg, 0.15 mmol); yield: 45 mg (76%); bright yellow solid; R_f = 0.67 (SiO_2; 2:1 hexanes/ethyl acetate); m.p. = 106–108 °C; ^{1}H NMR (400 MHz, $CDCl_3$, 298 K); δ = 7.74 (quasi d, J = 9.0 Hz, 2H), 7.71–7.64 (m, 3H), 7.63–7.53 (m, 4H), 6.98 (br. s, 1H), 4.27 (q, J = 7.1 Hz, 2H), 1.33 ppm (t, J = 7.1 Hz, 3H); $^{13}C\{^1H\}$ NMR (100 MHz, $CDCl_3$, 298 K); δ = 167.7, 165.6, 152.7, 144.6, 134.8, 131.5, 131.4, 130.2, 129.5, 125.3, 118.9, 112.3, 111.72, 111.68, 111.2, 87.9, 84.3, 62.4, 14.5 ppm; UV/vis (CH_2Cl_2): λ_{max} (ε) = 297 (2.21×10^4), 329 (2.37×10^4), 384 nm (1.98×10^4 M^{-1} cm^{-1}); IR (ATR): $\tilde{\nu}$ = 3335 (m), 2228 (m), 1716 (s) cm^{-1}; HRMS (ESI-TOF) m/z: $[M-H]^-$ Calcd. for $C_{23}H_{14}N_5O_2^-$ 392.1147; Found 392.1157.

Compound 15c: (Starting material **2c**: 40 mg, 0.14 mmol); yield: 55 mg (96%); bright yellow solid; R_f = 0.76 (SiO_2; 2:1 hexanes/ethyl acetate); m.p. = 126–128 °C; ^{1}H NMR (400 MHz, $CDCl_3$, 298 K); δ = 7.74 (d, J = 9.0 Hz, 2H), 7.71–7.66 (m, 3H), 7.62 (quasi d, J = 9.0 Hz, 2H), 7.57 (d, J = 8.0 Hz, 2 H), 7.06 (br. s, 1H), 3.99 (d, J = 6.7 Hz, 2H), 2.03–1.94 (m, 1H), 0.97 ppm (d, J = 6.7 Hz, 6H); $^{13}C\{^1H\}$ NMR (100 MHz, $CDCl_3$, 298 K); δ = 167.7, 165.6, 152.9, 144.6, 134.8, 131.5, 131.4, 130.2, 129.5, 125.2, 118.8, 112.3, 111.72, 111.68, 111.2, 87.8, 84.1, 72.3, 28.0, 19.1 ppm; UV/vis (CH_2Cl_2): λ_{max} (ε) = 295 (2.15×10^4), 330 (2.47×10^4), 386 nm (2.11×10^4 M^{-1} cm^{-1}); IR (ATR): $\tilde{\nu}$ = 3337 (m), 2228 (m), 1716 (s) cm^{-1}; HRMS (ESI-TOF) m/z: $[M-H]^-$ Calcd. for $C_{25}H_{18}N_5O_2^-$ 420.1461; Found 420.1454.

Compound 15d: (Starting material **2d**: 100 mg, 0.27 mmol); yield: 72 mg (53%); bright yellow solid; R_f = 0.38 (SiO_2; 3:2 hexanes/ethyl acetate); m.p. = 86–88 °C; ^{1}H NMR (400 MHz, $CDCl_3$, 298 K); δ = 7.75 (quasi d, J = 8.9 Hz, 2H), 7.71–7.64 (m, 5H), 7.60–7.54 (m, 2H), 7.39 (br. s, 1H), 4.85 ppm (s, 2H); $^{13}C\{^1H\}$ NMR (100 MHz, $CDCl_3$, 298 K); δ = 167.5, 165.7, 151.0, 143.5, 134.9, 131.4, 131.3, 130.2, 129.4, 126.0, 119.3, 112.1, 111.7, 111.5, 111.2, 94.8, 87.9, 85.2, 74.9 ppm; UV/vis (CH_2Cl_2): λ_{max} (ε) = 298 (2.02×10^4), 327 (2.17×10^4), 363 nm (1.88×10^4 M^{-1} cm^{-1}); IR (ATR): $\tilde{\nu}$ = 3319 (m), 2229 (m), 1749 (s) cm^{-1}; HRMS (ESI-TOF) m/z: $[M-H]^-$ Calcd. for $C_{23}H_{11}Cl_3N_5O_2^-$ 493.9978; Found 493.9971.

Compound 15e: (Starting material **2e**: 60 mg, 0.18 mmol); yield: 42 mg (50%); bright yellow solid; R_f = 0.49 (SiO_2; 2:1 hexanes/ethyl acetate; m.p. = 86–88 °C; ^{1}H NMR (400 MHz, $CDCl_3$, 298 K); δ = 7.75–7.53 (m, 10H), 7.41–7.37 (m, 4H), 7.05 (br. s, 1H), 5.23 ppm (s, 2H); $^{13}C\{^1H\}$ NMR (100 MHz, $CDCl_3$, 298 K); δ = 167.7, 165.6, 152.5, 144.3, 135.3, 134.8, 131.4, 130.2, 129.5, 128.9, 128.7, 125.4, 119.0, 112.3, 111.7, 111.6, 111.2, 87.9, 84.5, 68.1 ppm (20 out of 22 peaks observed); UV/vis (CH_2Cl_2): λ_{max} (ε) = 296 (1.40×10^4), 314 (1.39×10^4), 375 nm (1.07×10^4 M^{-1} cm^{-1}); IR (ATR): $\tilde{\nu}$ = 3329 (m), 2228 (m), 1734 (s) cm^{-1}; HRMS (ESI-TOF) m/z: $[M-H]^-$ Calcd. for $C_{28}H_{16}N_5O_2^-$ 454.1304; Found 454.1300.

Compound 16: (Starting material **2f**: 200 mg, 0.56 mmol); yield: 15 mg (8%); dark red solid; R_f = 0.39 (SiO_2; 2:1 hexanes/ethyl acetate; ^{1}H NMR (400 MHz, $CDCl_3$, 298 K); δ = 7.71 (d, J = 8.5 Hz, 4H), 7.67–7.62 (m, 1H), 7.55 (t, J = 7.7 Hz, 2H), 6.72 (d, J = 8.2 Hz, 2H), 4.70 ppm (br. s, 2H); IR (ATR): $\tilde{\nu}$ = 3316 (m), 2229 (m) cm^{-1}; Spectral data is consistent with the literature.[59]

Synthesis of Compound 18

4-Iodoaniline (**6**) (1.00 g, 4.57 mmol, 1.00 equiv.), CuI (17 mg, 0.09 mmol, 0.02 equiv.), $[Pd(PPh_3)_2Cl_2]$ (64 mg, 0.09 mmol, 0.02 equiv.), triphenylphosphine (48 mg, 0.18 mmol, 0.04 equiv.) was dissolved in 60 mL of DIPA/toluene mixture (1:5) in a flask sealed with a rubber septum. The system was purged with N_2 for 10 minutes. Subsequently, 1-ethynyl-4-methoxybenzene (**17**) (664 mg, 5.02 mmol, 1.10 equiv.) was introduced via syringe. The reaction mixture was stirred at room temperature overnight. After completion, the solvent was removed under reduced pressure, and the residue was extracted with CH_2Cl_2 (50 mL×2). The combined organic layers were dried over $MgSO_4$ and filtered. Following solvent removal and CC (SiO_2; hexanes/ethyl acetate, 3:1), compound **18** was obtained.

Compound 18: Yield: 653 mg (64%); red colored solid; R_f = 0.65 (SiO_2; 3:1 hexanes/ethyl acetate); ^{1}H NMR (400 MHz, $CDCl_3$, 298 K); δ = 7.43 (quasi d, J = 8.9 Hz, 2H), 7.32 (quasi d, J = 8.6 Hz, 2H), 6.86 (quasi d, J = 8.9 Hz, 2H), 6.63 (quasi d, J = 8.6 Hz, 2H), 3.82 (s, 3H), 3.79 ppm (br. s, 2H); $^{13}C\{^1H\}$ NMR (100 MHz, $CDCl_3$, 298 K); δ = 159.3, 146.5, 132.9 (2×C), 116.1, 114.9, 114.0, 113.1, 88.8, 87.3, 55.4 ppm. Spectral data is consistent with the literature.[95]

General procedure for the synthesis of 3a–f. Compound **18** (1.00 equiv.) was dissolved in 10 mL of THF and cooled using an ice bath. Pyridine (1.30 equiv.) was then added, followed by the dropwise addition of the corresponding chloroformates **7a–f** (1.20 equiv.). The reaction mixture was gradually warmed to room temperature and stirred for one hour. Upon completion, the reaction was quenched with water, extracted with CH_2Cl_2 (3×50 mL), and the combined organic layers were dried over $MgSO_4$. The solvent was removed under reduced pressure, and the resulting solid was purified by CC to afford products **3a–f**.[86]

Compound 3a: (Starting material **18**: 150 mg, 0.67 mmol); yield: 149 mg (79%); yellow solid; R_f = 0.83 (SiO_2; 2:1 hexanes/ethyl acetate); m.p. = 128–130 °C; ^{1}H NMR (400 MHz, $CDCl_3$, 298 K); δ = 7.48–7.43 ppm (m, 4H), 7.37 (quasi d, J = 8.3 Hz, 2H), 6.87 (quasi d, J = 8.7 Hz, 2H), 6.66 (br. s, 1H), 3.83 (s, 3H), 3.79 ppm (s, 3H); $^{13}C\{^1H\}$ NMR (100 MHz, $CDCl_3$, 298 K); δ = 159.6, 153.9, 137.7, 133.1, 132.4, 118.5, 118.4, 115.5, 114.1, 88.9, 87.9, 55.4, 52.6 ppm; IR (ATR): $\tilde{\nu}$ = 3360 (m), 1708 (s) cm^{-1}; HRMS (ESI-TOF) m/z: $[M+H]^+$ Calcd. for $C_{17}H_{16}NO_3^+$ 282.1130; Found 282.1129.

Compound 3b: (Starting material **18**: 250 mg, 1.12 mmol); yield: 307 mg (93%); yellow solid; R_f = 0.51 (SiO_2; CH_2Cl_2); m.p. = 150–152 °C; ^{1}H NMR (400 MHz, $CDCl_3$, 298 K); δ = 7.45 (quasi d, J = 8.6 Hz, 4H), 7.37 (quasi d, J = 8.6 Hz, 2H), 6.87 (quasi d, J = 8.6 Hz, 2H), 6.68 (br. s, 1H), 4.23 (q, J = 7.1 Hz, 2H), 3.82 (s, 3H), 1.32 ppm (t, J = 7.1 Hz, 3H); $^{13}C\{^1H\}$ NMR (100 MHz, $CDCl_3$, 298 K); δ = 159.6, 153.5, 137.9, 133.0, 132.4, 118.34, 118.30, 115.6, 114.1, 88.8, 87.9, 61.5, 55.4, 14.6 ppm; IR (ATR): $\tilde{\nu}$ = 3306 (m), 1703 (s) cm^{-1}. Spectral data is consistent with the literature.[96]

Compound 3c: (Starting material **18**: 129 mg, 0.58 mmol); yield: 173 mg (93%); yellow solid; (SiO_2; CH_2Cl_2); m.p. = 140–142 °C; ^{1}H NMR (400 MHz, $CDCl_3$, 298 K); δ = 7.45 (quasi d, J = 8.0 Hz, 4H), 7.37 (quasi d, J = 8.0 Hz, 2H), 6.87 (quasi d, J = 8.0 Hz, 2H), 6.72 (br. s, 1H), 3.96 (d, J = 6.6 Hz, 2H), 3.82 (s, 3H), 2.04–1.92 (m, 1H), 0.97 ppm (d, J = 6.6 Hz, 6H); $^{13}C\{^1H\}$ NMR (100 MHz, $CDCl_3$, 298 K); δ = 159.6, 153.6, 137.9, 133.1, 132.4, 118.4, 118.3, 115.6, 114.1, 88.8, 87.9, 71.7, 55.4, 28.1, 19.2 ppm; IR (ATR): $\tilde{\nu}$ = 3310 (m), 1701 (s) cm^{-1}; HRMS (ESI-TOF) m/z: $[M+H]^+$ Calcd. for $C_{20}H_{22}NO_3^+$ 324.1600; Found 324.1600.

Compound 3d: (Starting material **18**: 150 mg, 0.67 mmol); Yield: 223 mg (83%); yellow solid; R_f = 0.83 (SiO_2; 2:1 hexanes/ethyl acetate); m.p. = 142–144 °C; ^{1}H NMR (400 MHz, $CDCl_3$, 298 K); δ =

7.49 (quasi d, J = 8.7 Hz, 2H), 7.46 (quasi d, J = 8.7 Hz, 2H), 7.41 (quasi d, J = 8.7 Hz, 2H), 6.97 (br. s, 1H), 6.88 (quasi d, J = 8.7 Hz, 2H), 4.83 (s, 2H), 3.83 ppm (s, 3H); $^{13}C\{^1H\}$ NMR (100 MHz, $CDCl_3$, 298 K); δ = 159.7, 151.4, 136.8, 133.1, 132.5, 119.3, 118.6, 115.4, 114.1, 95.2, 89.3, 87.7, 74.6, 55.4 ppm; IR (ATR): $\tilde{\nu}$ = 3324 (m), 1714 (s) cm^{-1}; HRMS (ESI-TOF) m/z: $[M]^+$ Calcd. for $C_{18}H_{14}NO_3Cl_3^+$ 397.0039; Found 397.0038.

Compound 3e: (Starting material **18**: 250 mg, 1.12 mmol); yield: 352 mg (88%); yellow solid; R_f = 0.56 (SiO_2; 2:1 hexanes/ethyl acetate); m.p. = 148–150 °C; ^1H NMR (400 MHz, $CDCl_3$, 298 K); δ = 7.45 (quasi d, J = 8.8 Hz, 4H), 7.43–7.34 (m, 7H), 6.87 (quasi d, J = 8.8 Hz, 2H), 6.73 (br. s, 1H), 5.21 (s, 2H), 3.83 ppm (s, 3H); $^{13}C\{^1H\}$ NMR (100 MHz, $CDCl_3$, 298 K); δ = 159.6, 153.2, 137.6, 136.0, 133.1, 132.4, 128.8, 128.6, 128.5, 118.5, 118.4, 115.5, 114.1, 88.9, 87.9, 67.3, 55.4 ppm; IR (ATR): $\tilde{\nu}$ = 3300 (m), 1698 (s) cm^{-1}; HRMS (ESI-TOF) m/z: $[M + H]^+$ Calcd. for $C_{23}H_{20}NO_3^+$ 358.1443; Found 358.1444.

Compound 3f: (Starting material **18**: 150 mg, 0.67 mmol); yield: 206 mg (79%); yellow solid; R_f = 0.52 (SiO_2; CH_2Cl_2); decomposes at 188–190 °C; ^1H NMR (400 MHz, $CDCl_3$, 298 K); δ = 8.30 (quasi d, J = 9.2 Hz, 2H), 7.52 (quasi d, J = 8.7 Hz, 2H), 7.49–7.38 (m, 6H), 7.06 (br. s, 1H), 6.88 (quasi d, J = 8.8 Hz, 2H), 3.83 ppm (s, 3H); $^{13}C\{^1H\}$ NMR (100 MHz, $CDCl_3$, 298 K); δ = 159.8, 155.3, 145.3, 136.4, 133.2, 132.6, 126.4, 125.4, 122.3, 118.7, 115.8, 115.4, 114.2, 89.5, 87.6, 55.5 ppm; IR (ATR): $\tilde{\nu}$ = 3333 (m), 1731 (s) cm^{-1}; HRMS (ESI-TOF) m/z: $[M]^+$ Calcd. for $C_{22}H_{16}N_2O_5^+$ 388.1059; Found 388.1066.

General procedure for the synthesis of 19a–e and 20. A solution of compound **3a–f** (1.00 equiv.) in acetonitrile (10 mL) was prepared, and TCNE (1.50 equiv.) along with $LiClO_4$ (2.00 equiv.) was added under an inert atmosphere. The mixture was heated to 82 °C and stirred under an inert atmosphere for 3 days. The resulting product was purified by CC to yield the gel-like bright red solids **19a–e** in 19–57% yield and **20** in 8% yield.

Compound 19a: (Starting material **3a**: 100 mg, 0.36 mmol); yield: 61 mg (42%); bright red solid; R_f = 0.31 (SiO_2; 2:1 hexanes/ethyl acetate); m.p. = 154–156 °C; ^1H NMR (400 MHz, $CDCl_3$, 298 K); δ = 7.77 (quasi d, J = 8.9 Hz, 2H), 7.74 (quasi d, J = 8.9 Hz, 2H), 7.60 (quasi d, J = 8.9 Hz, 2H), 7.16 (br. s, 1H), 7.04 (quasi d, J = 8.9 Hz, 2H), 3.92 (s, 3H), 3.82 ppm (s, 3H); $^{13}C\{^1H\}$ NMR (100 MHz, $CDCl_3$, 298 K); δ = 166.4, 166.2, 165.2, 153.3, 144.4, 132.3, 131.5, 125.6, 123.7, 118.8, 115.8, 112.7, 112.5, 111.9, 111.7, 84.1, 83.0, 56.1, 53.2 ppm; UV/vis (CH_2Cl_2): λ_{max} (ε) = 260 (2.04×10^4), 384 nm (3.32×10^4 M^{-1} cm^{-1}); IR (ATR): $\tilde{\nu}$ = 3334 (m), 2226 (s), 1739 (s) cm^{-1}; HRMS (ESI-TOF) m/z: $[M-H]^-$ Calcd. for $C_{23}H_{14}N_5O_3^-$ 408.1097; Found 408.1095.

Compound 19b: (Starting material **3b**: 50 mg, 0.17 mmol); yield: 41 mg (57%); bright red solid; R_f = 0.58 (SiO_2; 1:1 hexanes/ethyl acetate); m.p. = 142–144 °C; ^1H NMR (400 MHz, $CDCl_3$, 298 K); δ = 7.76 (quasi d, J = 8.9 Hz, 2H), 7.74 (quasi d, J = 8.9 Hz, 2H), 7.59 (quasi d, J = 8.9 Hz, 2H), 7.13 (br. s, 1H), 7.03 (quasi d, J = 8.9 Hz, 2H), 4.26 (q, J = 7.1 Hz, 2H), 3.91 (s, 3H), 1.32 ppm (t, J = 7.1 Hz, 3H); $^{13}C\{^1H\}$ NMR (100 MHz, $CDCl_3$, 298 K); δ = 166.3, 166.2, 165.2, 152.8, 144.6, 132.3, 131.5, 125.5, 123.7, 118.8, 115.8, 112.7, 112.5, 111.9, 111.8, 83.9, 83.1, 62.3, 56.1, 14.5 ppm; UV/vis (CH_2Cl_2): λ_{max} (ε) = 266 (1.93×10^4), 384 nm (3.02×10^4 M^{-1} cm^{-1}); IR (ATR): $\tilde{\nu}$ = 3327 (m), 2227 (s), 1715 (s) cm^{-1}; HRMS (ESI-TOF) m/z: $[M-H]^-$ Calcd. for $C_{24}H_{16}N_5O_3^-$ 422.1253; Found 422.1253.

Compound 19c: (Starting material **3c**: 100 mg, 0.31 mmol); yield: 57 mg (41%); bright red solid; R_f = 0.32 (SiO_2; 2:1 hexanes/ethyl acetate); ^1H NMR (400 MHz, $CDCl_3$, 298 K); δ = 7.79–7.72 (m, 4H), 7.60 (d, J = 9.0 Hz, 2H), 7.13 (br. s, 1H), 7.04 (d, J = 9.1 Hz, 2H), 3.98 (d, J = 6.7 Hz, 2H), 3.91 (s, 3H), 2.03–1.94 (m, 1H), 0.97 ppm (d, J = 6.7 Hz, 6H); $^{13}C\{^1H\}$ NMR (100 MHz, $CDCl_3$, 298 K); δ = 166.34, 166.26, 165.2, 152.9, 144.6, 132.3, 131.5, 125.5, 123.7, 118.8, 115.8, 112.7, 112.5, 111.9, 111.7, 83.9, 83.0, 72.3, 56.1, 28.0, 19.1 ppm; UV/vis (CH_2Cl_2): λ_{max} (ε) = 260 (2.24×10^4), 384 nm (3.61×10^4 M^{-1} cm^{-1}); IR (ATR): $\tilde{\nu}$ = 3334 (m), 2227 (s), 1714 (s) cm^{-1}; HRMS (ESI-TOF) m/z: $[M-H]^-$ Calcd. for $C_{26}H_{20}N_5O_3^-$ 450.1566; Found 450.1567.

Compound 19d: (Starting material **3d**: 100 mg, 0.25 mmol); yield: 25 mg (19%); bright red solid; R_f = 0.58 (SiO_2; 1:1 hexanes/ethyl acetate); m.p. = 105–107 °C; ^1H NMR (400 MHz, $CDCl_3$, 298 K); δ = 7.79–7.75 (m, 4H), 7.65 (quasi d, J = 8.9 Hz, 2H), 7.29 (br. s, 1H), 7.05 (quasi d, J = 8.9 Hz, 2H), 4.85 (s, 2H), 3.92 ppm (s, 3H); $^{13}C\{^1H\}$ NMR (100 MHz, $CDCl_3$, 298 K); δ = 166.4, 166.0, 165.3, 151.0, 143.4, 132.3, 131.4, 126.4, 123.6, 119.2, 115.9, 112.6, 112.3, 111.9, 111.5, 94.8, 85.0, 83.1, 74.9, 56.1 ppm; UV/vis (CH_2Cl_2): λ_{max} (ε) = 270 (1.62×10^4), 378 nm (2.21×10^4 M^{-1} cm^{-1}); IR (ATR): $\tilde{\nu}$ = 3310 (m), 2227 (s), 1751 (s) cm^{-1}; HRMS (ESI-TOF) m/z: $[M-H]^-$ Calcd. for $C_{24}H_{13}N_5O_3Cl_3^-$ 524.0084; Found 524.0084.

Compound 19e: (Starting material **3e**: 100 mg, 0.28 mmol); yield: 75 mg (55%); bright red solid; R_f = 0.31 (SiO_2; 2:1 hexanes/ethyl acetate); m.p. = 93–95 °C; ^1H NMR (400 MHz, $CDCl_3$, 298 K); δ = 7.78–7.71 (m, 4H), 7.59 (quasi d, J = 8.9 Hz, 2H), 7.41–7.37 (m, 5H), 7.07 (br. s, 1H), 7.04 (quasi d, J = 8.9 Hz, 2H), 5.23 (s, 2H), 3.92 ppm (s, 3H); $^{13}C\{^1H\}$ NMR (100 MHz, $CDCl_3$, 298 K); δ = 166.3, 166.2, 165.2, 152.6, 144.3, 135.3, 132.2, 131.4, 128.82, 128.79, 128.5, 125.6, 123.6, 118.8, 115.8, 112.6, 112.5, 111.9, 111.7, 84.0, 83.0, 67.9, 56.1 ppm; UV/vis (CH_2Cl_2): λ_{max} (ε) = 268 (1.93×10^4), 382 nm (2.40×10^4 M^{-1} cm^{-1}); IR (ATR): $\tilde{\nu}$ = 3310 (m), 2226 (s), 1734 (s) cm^{-1}; HRMS (ESI-TOF) m/z: $[M-H]^-$ Calcd. for $C_{29}H_{18}N_5O_3^-$ 484.1410; Found 484.1409.

Compound 20: (Starting material **3f**: 90 mg, 0.23 mmol); yield: 6.8 mg (8%); bright red solid; R_f = 0.28 (SiO_2; 1:1 hexanes/ethyl acetate); m.p. = 96–98 °C; ^1H NMR (400 MHz, $CDCl_3$, 298 K); δ = 7.78 (d, J = 9.0 Hz, 2H), 7.70 (quasi d, J = 8.9 Hz, 2H), 7.02 (quasi d, J = 9.0 Hz, 2H), 6.70 (quasi d, J = 8.9 Hz, 2H), 4.68 (br. s, 2H), 3.91 ppm (s, 3H); ^{13}C NMR (100 MHz, $CDCl_3$, 298 K); δ = 167.4, 165.3, 165.0, 153.3, 132.9, 132.4, 124.2, 120.6, 115.6, 115.1, 113.8, 112.9, 112.8, 112.0, 83.0, 78.0, 56.0 ppm; IR (ATR): $\tilde{\nu}$ = 3362 (m), 2220 (s) cm^{-1}; HRMS (ESI-TOF) m/z: $[M-H]^-$ Calcd. for $C_{21}H_{12}N_5O^-$ 350.1042; Found 350.1037.

Synthesis of compound 22: In a flask sealed with a rubber septum, 4-iodoaniline (**6**) (474 mg, 2.16 mmol, 1.00 equiv.), CuI (8 mg, 0.04 mmol, 0.02 equiv.), $[Pd(PPh_3)_2Cl_2]$ (30 mg, 0.04 mmol, 0.02 equiv.), and triphenylphosphine (23 mg, 0.09 mmol, 0.04 equiv.) were dissolved in a 30 mL mixture of DIPA and toluene (1:5). The atmosphere was purged with N_2 for 10 minutes. Subsequently, 4-ethynyl-*N*,*N*-diethylaniline (**21**) (450 mg, 2.60 mmol, 1.20 equiv.) was added via syringe. The reaction mixture was stirred at 60 °C for 3 days. Upon completion, the solvent was removed under reduced pressure, and the residue was extracted with CH_2Cl_2 (50 mL×2). The combined organic layers were dried over $MgSO_4$ and filtered. Evaporation of the solvent, followed by purification via CC (SiO_2; CH_2Cl_2), gave product **22**.[90]

Compound 22: Yield: 450 mg (79%); R_f = 0.47 (SiO_2; CH_2Cl_2); m.p. = 90–92 °C; ^1H NMR (400 MHz, $CDCl_3$, 298 K): δ = 7.34 (quasi d, J = 8.9 Hz, 2H), 7.30 (quasi d, J = 8.9 Hz, 2H), 6.62 (quasi d, J = 8.9 Hz, 4H), 3.76 (br. s, 2H), 3.36 (q, J = 7.1 Hz, 4H), 1.17 ppm (t, J = 7.1 Hz, 6H); ^{13}C NMR (100 MHz, $CDCl_3$, 298 K): δ = 147.2, 146.1, 132.7, 132.6, 114.9, 113.7, 111.4, 109.7, 88.4, 87.5, 44.4, 12.6 ppm; IR (ATR): $\tilde{\nu}$ = 3447 (m), 3352 (m), 2203 (m) cm^{-1}; HRMS (ESI-TOF) m/z: $[M + H]^+$ Calcd. for $C_{18}H_{21}N_2^+$ 265.1705; Found 265.1705.

General procedure for the synthesis of 4a–f. Compound **22** (1.00 equiv.) was dissolved in 10 mL of THF and cooled using an ice bath. Pyridine (1.30 equiv.) was then added, followed by the dropwise addition of the corresponding chloroformates **7a–f** (1.20 equiv.). The reaction mixture was gradually warmed to room temperature and stirred for one hour. Upon completion, the reaction was quenched with water, extracted with CH_2Cl_2

(3×30 mL), and the combined organic layers were dried over $MgSO_4$. The solvent was removed under reduced pressure, and the resulting solid was purified by CC to afford products **4a–f** in 43–91% yield[86]

Compound 4a: (Starting material **22**: 140 mg, 0.53 mmol); yield: 131 mg (77%); grey solid; R_f = 0.52 (SiO_2; 1:1 hexanes/ethyl acetate); m.p. = 156–158 °C; ^{1}H NMR (400 MHz, $CDCl_3$, 298 K); δ = 7.44 (quasi d, J = 8.6 Hz, 2H), 7.38–7.32 (m, 4H), 6.65 (br. s, 1H), 6.60 (quasi d, J = 8.9 Hz, 2H), 3.78 (s, 3H), 3.37 (q, J = 7.1 Hz, 4H), 1.17 ppm (t, J = 7.1 Hz, 6H); ^{13}C{^{1}H} NMR (100 MHz, $CDCl_3$, 298 K.); δ = 154.0, 147.5, 137.2, 132.9, 132.1, 119.2, 118.4, 111.3, 109.0, 90.2, 86.9, 52.5, 44.4, 12.6 ppm; IR (ATR): $\tilde{\nu}$ = 3334 (m), 2203 (m), 1702 (s) cm^{-1}; HRMS (ESI-TOF) m/z: [M + H]$^+$ Calcd. for $C_{20}H_{23}N_2O_2^+$ 323.1760; Found 323.1755.

Compound 4b: (Starting material **22**: 210 mg, 0.79 mmol); yield: 217 mg (81%); grey solid; R_f = 0.44 (SiO_2; 5:2 hexanes/ethyl acetate); m.p. = 123–125 °C; ^{1}H NMR (400 MHz, $CDCl_3$, 298 K); δ = 7.43 ppm (quasi d, J = 8.8 Hz, 2H), 7.37–7.32 (m, 4H), 6.62 (br. s, 1H), 6.60 (quasi d, J = 8.8 Hz, 2H), 4.23 (q, J = 7.1 Hz, 2H), 3.37 (q, J = 7.0 Hz, 4H), 1.31 (t, J = 7.1 Hz, 3H), 1.17 ppm (t, J = 7.0 Hz, 6H); ^{13}C{^{1}H} NMR (100 MHz, $CDCl_3$, 298 K); δ = 153.5, 147.5, 137.3, 133.0, 132.2, 119.1, 118.3, 111.3, 109.1, 90.2, 86.9, 61.5, 44.4, 14.7, 12.7 ppm; IR (ATR): $\tilde{\nu}$ = 3340 (m), 2203 (m), 1704 (s) cm^{-1}; HRMS (ESI-TOF) m/z: [M + H]$^+$ Calcd. for $C_{21}H_{25}N_2O_2^+$ 337.1916; Found 337.1909.

Compound 4c: (Starting material **22**: 450 mg, 1.70 mmol); yield: 564 mg (91%); grey solid; R_f = 0.78 (SiO_2; CH_2Cl_2); m.p. = 159–161 °C; ^{1}H NMR (400 MHz, $CDCl_3$, 298 K); δ = 7.44 (quasi d, J = 8.9 Hz, 2H), 7.38–7.34 (m, 4H), 6.63 (br. s, 1H), 6.60 (quasi d, J = 8.9 Hz, 2H), 3.95 (d, J = 6.7 Hz, 2H), 3.37 (q, J = 7.0 Hz, 4H), 2.04–1.92 (m, 1H), 1.17 (t, J = 7.0 Hz, 6H), 0.97 ppm (d, J = 6.7 Hz, 6H); ^{13}C{^{1}H} NMR (100 MHz, $CDCl_3$, 298 K); δ = 153.6, 147.5, 137.3, 132.9, 132.1, 119.1, 118.3, 111.2, 109.0, 90.2, 86.9, 71.5, 44.4, 28.0, 19.1, 12.6 ppm; IR (ATR): $\tilde{\nu}$ = 3336 (m), 2203 (m), 1702 (s) cm^{-1}; HRMS (ESI-TOF) m/z: [M + H]$^+$ Calcd. for $C_{23}H_{29}N_2O_2^+$ 365.2229; Found 365.2229.

Compound 4d: (Starting material **22**: 40 mg, 1.15 mmol); yield: 55 mg (83%); grey solid; R_f = 0.75 (SiO_2; 5:2 hexanes/ethyl acetate); m.p. = 171–173 °C; ^{1}H NMR (400 MHz, $CDCl_3$, 298 K); δ = 7.47 (quasi d, J = 8.4 Hz, 2H), 7.43–7.33 (m, 4H), 6.91 (br. s, 1H), 6.61 (quasi d, J = 8.6 Hz, 2H), 4.83 (s, 2H), 3.37 (q, J = 7.0 Hz, 4H), 1.17 ppm (t, J = 7.0 Hz, 6H); ^{13}C{^{1}H} NMR (100 MHz, $CDCl_3$, 298 K); δ = 151.4, 147.6, 136.2, 133.0, 132.3, 120.2, 118.6, 111.3, 108.9, 95.3, 90.7, 86.7, 74.7, 44.5, 12.7 ppm; IR (ATR): $\tilde{\nu}$ = 3336 (m), 2208 (s), 1719 (s) cm^{-1}; HRMS (ESI-TOF) m/z: [M + H]$^+$ Calcd. for $C_{21}H_{22}N_2O_2Cl_3^+$ 439.0747; Found 439.0748.

Compound 4e: (Starting material **22**: 153 mg, 0.58 mmol); yield: 135 mg (59%); grey solid; R_f = 0.58 (SiO_2; 5:2 hexanes/ethyl acetate); m.p. = 127–129 °C; ^{1}H NMR (400 MHz, $CDCl_3$, 298 K); δ = 7.33–7.45 (m, 11H), 6.72 (br. s, 1H), 6.61 (d, J = 8.9 Hz, 2H), 5.21 (s, 2H), 3.37 (q, J = 7.0 Hz, 4H), 1.18 ppm (t, J = 7.0 Hz, 6H); ^{13}C{^{1}H} NMR (100 MHz, $CDCl_3$, 298 K); δ = 153.2, 147.6, 137.1, 136.1, 133.0, 132.2, 128.8, 128.6, 128.5, 119.5, 118.5, 111.4, 109.2, 90.4, 86.9, 67.3, 44.5, 12.7 ppm; IR (ATR): $\tilde{\nu}$ = 3385 (m), 2207 (m), 1744 (s) cm^{-1}; HRMS (ESI-TOF) m/z: [M + H]$^+$ Calcd. for $C_{26}H_{27}N_2O_2^+$ 399.2073; Found 399.2078.

Compound 4f: (Starting material **22**: 177 mg, 0.67 mmol); yield: 123 mg (43%); grey solid; R_f = 0.50 (SiO_2; 5:2 hexanes/ethyl acetate); m.p. = 142–144 °C; ^{1}H NMR (400 MHz, $CDCl_3$, 298 K); δ = 8.29 (quasi d, J = 9.1 Hz, 2H), 7.49 (quasi d, J = 8.5 Hz, 2H), 7.42–7.36 (m, 6H), 7.05 (br. s, 1H), 6.61 (quasi d, J = 8.5 Hz, 2H), 3.37 (q, J = 7.0 Hz, 4H), 1.17 ppm (t, J = 7.0 Hz, 6H); ^{13}C{^{1}H} NMR (100 MHz, $CDCl_3$, 298 K); δ = 155.4, 150.1, 147.7, 145.2, 138.3, 135.9, 133.0, 132.3, 125.3, 122.3, 118.8, 111.3, 108.7, 91.0, 86.6, 44.4, 12.7 ppm; IR (ATR): $\tilde{\nu}$ = 3273 (m), 2206 (m), 1723 (s) cm^{-1}; HRMS (ESI-TOF) m/z: [M + H]$^+$ Calcd. for $C_{25}H_{24}N_3O_4^+$ 430.1767; Found 430.1767.

General procedure for the synthesis of 23a–e and 24. A solution of compounds **4a–f** (1.00 equiv.) in dichloromethane (2 mL) was prepared, and TCNE (**11**) (1.00 equiv.) was added. The mixture was stirred for 15 minutes, then purified by CC to yield dark red solids **23a–e** in 88–98% yield and **24** in 63% yield.

Compound 23a: (Starting material **4a**: 27 mg, 0.08 mmol); yield: 33 mg (88%); dark red solid; R_f = 0.33 (SiO_2; 1:1 hexanes/ethyl acetate); m.p. = 154–156 °C; ^{1}H NMR (400 MHz, $CDCl_3$, 298 K); δ = 7.79–7.74 (m, 4H), 7.56 (quasi d, J = 8.3 Hz, 2H), 7.12 (br. s, 1H), 6.70 (quasi d, J = 8.8 Hz, 2H), 3.81 (s, 3H), 3.49 (q, J = 6.8 Hz, 4H), 1.25 ppm (t, J = 6.8 Hz, 6H); ^{13}C{^{1}H} NMR (100 MHz, $CDCl_3$, 298 K); δ = 168.0, 163.2, 153.4, 152.8, 144.2, 133.1, 131.5, 126.2, 118.6, 117.8, 114.7, 113.9, 112.9, 112.2, 112.0, 83.6, 73.0, 53.1, 45.3, 12.7 ppm; UV/vis (CH_2Cl_2): λ_{max} (ε) = 386 (3.58×10^4), 475 nm (4.47×10^4 M^{-1} cm^{-1}); IR (ATR): $\tilde{\nu}$ = 3339 (m), 2232 (m), 1736 (s) cm^{-1}; HRMS (ESI-TOF) m/z: [M + H]$^+$ Calcd. for $C_{26}H_{23}N_6O_2^+$ 451.1882; Found 451.1884.

Compound 23b: (Starting material **4b**: 70 mg, 0.21 mmol); yield: 92 mg (95%); dark red solid; R_f = 0.48 (SiO_2; 1:1 hexanes/ethyl acetate); m.p. = 204–206 °C; ^{1}H NMR (400 MHz, $CDCl_3$, 298 K); δ = 7.77 (quasi d, J = 9.0 Hz, 4H), 7.56 (quasi d, J = 9.0 Hz, 2H), 6.93 (br. s, 1H), 6.70 (quasi d, J = 9.0 Hz, 2H), 4.26 (q, J = 7.1 Hz, 2H), 3.49 (q, J = 7.1 Hz, 4H), 1.33 (t, J = 7.1 Hz, 3H), 1.25 ppm (t, J = 7.1 Hz, 6H); ^{13}C{^{1}H} NMR (100 MHz, $CDCl_3$, 298 K); δ = 168.1, 162.9, 152.9, 151.0, 143.1, 133.0, 131.5, 127.0, 119.0, 117.7, 114.7, 113.8, 112.7, 112.2, 111.8, 94.9, 84.6, 74.9, 73.1, 45.3, 12.7 ppm; UV/vis (CH_2Cl_2): λ_{max} (ε) = 387 (3.03×10^4), 475 nm (3.65×10^4 M^{-1} cm^{-1}); IR (ATR): $\tilde{\nu}$ = 3295 (m), 2218 (s), 1735 (s) cm^{-1}; HRMS (ESI-TOF) m/z: [M + H]$^+$ Calcd. for $C_{27}H_{25}N_6O_2^+$ 465.2039; Found 465.2039.

Compound 23c: (Starting material **4c**: 289 mg, 0.79 mmol); yield: 362 mg (93%); dark red solid; R_f = 0.61 (SiO_2; 1:1 hexanes/ethyl acetate); m.p. = 130–132 °C; ^{1}H NMR (400 MHz, $CDCl_3$, 298 K); δ = 7.79–7.75 (m, 4H), 7.57 (quasi d, J = 8.8 Hz, 2H), 6.95 (br. s, 1H), 6.72 (quasi d, J = 8.8 Hz, 2H), 3.98 (d, J = 6.6 Hz, 2H), 3.49 (q, J = 7.1 Hz, 4H), 2.03–1.94 (m, 1H), 1.26 (t, J = 7.1 Hz, 6H), 0.97 ppm (d, J = 6.6 Hz, 6H); ^{13}C{^{1}H} NMR (100 MHz, $CDCl_3$, 298 K); δ = 168.0, 163.2, 153.0, 152.8, 144.3, 133.0, 131.5, 126.1, 118.6, 117.7, 114.8, 113.8, 112.9, 112.1, 112.0, 83.5, 73.0, 72.2, 45.3, 28.0, 19.1, 12.7 ppm; UV/vis (CH_2Cl_2): λ_{max} (ε) = 388 (2.68×10^4), 476 nm (3.27×10^4 M^{-1} cm^{-1}); IR (ATR): $\tilde{\nu}$ = 3317 (m), 2214(s), 1736 (m) cm^{-1}; HRMS (ESI-TOF) m/z: [M + H]$^+$ Calcd. for $C_{29}H_{29}N_6O_2^+$ 493.2352; Found 493.2352.

Compound 23d: (Starting material **4d**: 53 mg, 0.12 mmol); yield: 60 mg (88%); deep red solid; R_f = 0.22 (SiO_2; 2:1 hexanes/ethyl acetate); m.p. = 160–162 °C; ^{1}H NMR (400 MHz, $CDCl_3$, 298 K); δ = 7.81–7.75 (m, 4H), 7.62 (quasi d, J = 8.8 Hz, 2H), 7.30 (br. s, 1H), 6.72 (quasi d, J = 9.2 Hz, 2H), 4.85 (s, 2H), 3.49 (q, J = 7.0 Hz, 4H), 1.26 ppm (t, J = 7.0 Hz, 6H); ^{13}C{^{1}H} NMR (100 MHz, $CDCl_3$, 298 K); δ = 168.1, 162.9, 152.9, 151.0, 143.1, 133.0, 131.5, 127.0, 119.0, 117.7, 114.7, 113.8, 112.7, 112.2, 111.8, 94.9, 84.6, 74.9, 73.1, 45.3, 12.7 ppm; UV/vis (CH_2Cl_2): λ_{max} (ε) = 376 (2.57×10^4), 475 nm (3.35×10^4 M^{-1} cm^{-1}); IR (ATR): $\tilde{\nu}$ = 3300 (m), 2213 (m), 1748 (m) cm^{-1}; HRMS (ESI-TOF) m/z: [M + H]$^+$ Calcd. for $C_{27}H_{22}Cl_3N_6O_2^+$ 567.0870; Found 567.0871.

Compound 23e: (Starting material **4e**: 37 mg, 0.09 mmol); yield: 48 mg (98%); deep red solid; R_f = 0.41 (SiO_2; 1:1 hexanes/ethyl acetate); m.p. = 209–211 °C; ^{1}H NMR (400 MHz, $CDCl_3$, 298 K); δ = 7.78–7.74 (m, 4H), 7.56 (quasi d, J = 8.7 Hz, 2H), 7.41–7.38 (m, 5H), 7.04 (br. s, 1H), 6.71 (quasi d, J = 9.2 Hz, 2H), 5.22 (s, 2H), 3.49 (q, J = 7.0 Hz, 4H), 1.25 ppm (t, J = 7.0 Hz, 6H); ^{13}C{^{1}H} NMR (100 MHz, $CDCl_3$, 298 K); δ = 168.0, 163.1, 152.8, 152.7, 144.0, 135.5, 133.0, 131.5, 128.83, 128.76, 128.5, 126.3, 118.7, 117.7, 114.7, 113.9, 112.8, 112.1, 112.0, 83.8, 73.1, 67.8, 45.3, 12.7 ppm; UV/vis (CH_2Cl_2): λ_{max}

(ε) = 386 (2.49×10⁴), 475 nm (3.05×10⁴ M^{-1} cm^{-1}); IR (ATR): $\tilde{\nu}$ = 3313 (m), 2213 (s), 1742 (s) cm^{-1}; HRMS (ESI-TOF) m/z: $[M + H]^+$ Calcd. for $C_{32}H_{27}N_6O_2^+$ 527.2195; Found 527.2194.

Compound 24: (Starting material **4f**: 47 mg, 0.11 mmol); yield: 27 mg (63%); deep red solid; R_f = 0.31 (SiO_2; 1:1 hexanes/ethyl acetate); m.p. = 217–219 °C; ^1H NMR (400 MHz, $CDCl_3$, 298 K); δ = 7.77 (quasi d, J = 9.3 Hz, 2H), 7.70 (quasi d, J = 8.9 Hz, 2H), 6.69–6.63 (m, 4H), 4.65 (br. s, 2H), 3.47 (q, J = 7.1 Hz, 4H), 1.24 ppm (t, J = 7.1 Hz, 6H); $^{13}C\{^1H\}$ NMR (100 MHz, $CDCl_3$, 298 K); δ = 167.0, 164.5, 153.0, 152.7, 133.1, 132.9, 121.3, 118.3, 114.93, 114.86, 114.1, 113.9, 113.0, 112.0, 78.1, 73.7, 45.2, 12.7 ppm; UV/vis (CH_2Cl_2): λ_{max} (ε) = 426 (2.95×10⁴), 474 nm (3.29×10⁴ M^{-1} cm^{-1}); IR (ATR): $\tilde{\nu}$ = 3469 (m), 3365 (m), 2210 (s) cm^{-1}; HRMS (ESI-TOF) m/z: $[M + H]^+$ Calcd. for $C_{24}H_{21}N_6^+$ 393.1828; Found 393.1828.

General procedure for the synthesis of 26a–e and **27**. A solution of compounds **4a–f** (1.00 equiv.) in dichloromethane (2 mL) was treated with TCNQ (**25**) (1.00 equiv.) and stirred for 1.5 hours. The reaction mixture was then purified by CC, yielding dark blue solids **26a–e** in 78–94 yields and **27** in 59% yield.

Compound 26a: (Starting material **4a**: 27 mg, 0.08 mmol); yield: 38 mg; dark green solid; 86%; R_f = 0.55 (SiO_2; 1:1 hexanes/ethyl acetate); m.p. = 220–222 °C; ^1H NMR (400 MHz, $CDCl_3$, 298 K); δ = 7.68 (quasi d, J = 8.7 Hz, 2H), 7.57–7.50 (m, 3H), 7.31–7.25 (m, 3H), 7.12 (quasi d, J = 7.7 Hz, 2H), 6.93 (d, J = 9.3 Hz, 1H), 6.71 (quasi d, J = 8.7 Hz, 2H), 3.79 (s, 3H), 3.47 (q, J = 7.0 Hz, 4H), 1.24 ppm (t, J = 7.0 Hz, 6H); $^{13}C\{^1H\}$ NMR (100 MHz, $CDCl_3$, 298 K); δ = 171.5, 154.4, 153.5, 152.6, 151.1, 143.6, 136.0, 135.1, 134.6, 131.6, 131.2, 128.9, 125.0, 124.6, 123.6, 118.6, 115.31, 115.26, 113.6, 112.82, 112.75, 84.5, 69.9, 53.0, 45.3, 12.7 ppm; UV/vis (CH_2Cl_2): λ_{max} (ε) = 465 (1.94×10⁴), 690 nm (4.86×10⁴ M^{-1} cm^{-1}); IR (ATR): $\tilde{\nu}$ = 3287 (m), 2195 (s), 2170 (s), 1733 (s) cm^{-1}; HRMS (ESI-TOF) m/z: $[M + H]^+$ Calcd. for $C_{32}H_{27}N_6O_2^+$ 527.2195; Found 527.2195.

Compound 26b: (Starting material **4b**: 40 mg, 0.12 mmol); yield: 60 mg (93%); dark green solid; R_f = 0.48 (SiO_2; 1:1 hexanes/ethyl acetate); m.p. = 230–232 °C; ^1H NMR (400 MHz, $CDCl_3$, 298 K); δ = 7.68 (quasi d, J = 8.8 Hz, 2H), 7.55–7.47 (m, 3H), 7.31–7.24 (m, 3H), 7.13 (dd, J = 9.5, 1.6 Hz, 1H), 6.98–6.88 (m, 2H), 6.74 (d, J = 8.4 Hz, 2H), 4.23 (q, J = 7.1 Hz, 2H), 3.47 (q, J = 7.1 Hz, 4H), 1.31 (t, J = 7.1 Hz, 3H), 1.25 ppm (t, J = 7.1 Hz, 6H); $^{13}C\{^1H\}$ NMR (100 MHz, $CDCl_3$, 298 K); δ = 171.5, 154.4, 153.0, 152.6, 151.2, 143.6, 136.0, 135.1, 134.6, 131.6, 131.1, 128.9, 125.0, 124.6, 123.5, 118.6, 115.3, 115.2, 113.6, 112.8, 112.7, 84.5, 70.0, 62.1, 45.3, 14.5, 12.7 ppm; UV/vis (CH_2Cl_2): λ_{max} (ε) = 466 (1.66×10⁴), 690 nm (4.19×10⁴ M^{-1} cm^{-1}); IR (ATR): $\tilde{\nu}$ = 3347 (m), 2195 (s), 1729 (s) cm^{-1}; HRMS (ESI-TOF) m/z: $[M + H]^+$ Calcd. for $C_{33}H_{29}N_6O_2^+$ 541.2352; Found 541.2350.

Compound 26c: (Starting material **4c**: 200 mg, 0.59 mmol); yield: 242 mg (78%); dark green solid; R_f = 0.40 (SiO_2; 1:1 hexanes/ethyl acetate); m.p. = 186–188 °C; ^1H NMR (400 MHz, $CDCl_3$, 298 K); δ = 7.69 (quasi d, J = 8.8 Hz, 2H), 7.54–7.47 (m, 3H), 7.31–7.25 (m, 3H), 7.13 (dd, J = 9.5, 1.5 Hz, 1H), 6.99–6.90 (m, 2H), 6.76 (quasi d, J = 7.5 Hz, 2H), 3.96 (d, J = 6.7 Hz, 2H), 3.47 (q, J = 7.0 Hz, 4H), 2.03–1.91 (m, 1H), 1.25 (t, J = 7.0 Hz, 6H), 0.95 ppm (d, J = 6.7 Hz, 6H); $^{13}C\{^1H\}$ NMR (100 MHz, $CDCl_3$, 298 K); δ = 171.5, 154.4, 153.1, 152.6, 151.2, 143.7, 136.0, 135.1, 134.6, 131.6, 131.1, 128.9, 125.0, 124.6, 123.5, 118.5, 115.3, 115.2, 113.6, 112.8, 112.6, 84.5, 72.1, 70.0, 45.3, 28.0, 19.1, 12.7 ppm; UV/vis (CH_2Cl_2): λ_{max} (ε) = 466 (1.99×10⁴), 692 nm (5.26×10⁴ M^{-1} cm^{-1}); IR (ATR): $\tilde{\nu}$ = 3264 (m), 2202 (s), 1732 (s) cm^{-1}; HRMS (ESI-TOF) m/z: $[M + H]^+$ Calcd. for $C_{35}H_{33}N_6O_2^+$ 569.2665; Found 569.2667.

Compound 26d: (Starting material **4d**: 65 mg, 0.15 mmol); yield: 89 mg; dark green solid; 94%; R_f = 0.46 (SiO_2; 1:1 hexanes/ethyl acetate); m.p. = 200 °C (decomp.); ^1H NMR (400 MHz, $CDCl_3$, 298 K); δ = 7.71 (quasi d, J = 8.8 Hz, 2H), 7.59–7.53 (m, 2H), 7.52 (dd, J = 9.5, 1.5 Hz, 1H), 7.33–7.26 (m, 3H), 7.25 (br. s, 1H), 7.13 (dd, J = 9.5, 1.7 Hz, 1H), 6.92 (dd, J = 9.4, 1.5 Hz, 1H), 6.69 (quasi d, J = 9.1 Hz, 2H), 4.82 (s, 2H), 3.47 (q, J = 7.0 Hz, 4H), 1.25 ppm (t, J = 7.0 Hz, 6H); $^{13}C\{^1H\}$ NMR (100 MHz, $CDCl_3$, 298 K); δ = 171.5, 154.3, 152.0, 151.2, 151.1, 142.3, 135.9, 135.0, 134.4, 131.6, 131.4, 130.0, 125.3, 124.9, 123.5, 119.0, 115.1, 115.0, 113.5, 112.6, 94.9, 89.8, 85.6, 74.9, 71.0, 45.3, 12.8 ppm; UV/vis (CH_2Cl_2): λ_{max} (ε) = 468 (1.48×10⁴), 692 nm (3.72×10⁴ M^{-1} cm^{-1}); IR (ATR): $\tilde{\nu}$ = 3287 (m), 2195 (s), 2170 (s), 1733 (s) cm^{-1}; HRMS (ESI-TOF) m/z: $[M-H]^-$ Calcd. for $C_{33}H_{24}Cl_3N_6O_2^-$ 641.1026; Found 641.1024.

Compound 26e: (Starting material **4e**: 37 mg, 0.09 mmol); yield: 46 mg (82%); dark green solid; R_f = 0.41 (SiO_2; 1:1 hexanes/ethyl acetate); m.p. = 175–177 °C; ^1H NMR (400 MHz, $CDCl_3$, 298 K); δ = 7.68 (quasi d, J = 8.5 Hz, 2H), 7.55–7.46 (m, 3H), 7.43–7.35 (m, 5H), 7.35–7.25 (m, 3H), 7.14 (d, J = 9.8 Hz, 1H), 7.03 (br. s, 1H), 6.93 (d, J = 9.3 Hz, 1H), 6.79 (quasi d, J = 7.9 Hz, 2H), 5.20 (s, 2H), 3.47 (q, J = 7.0 Hz, 4H), 1.25 ppm (t, J = 7.0 Hz, 6H); $^{13}C\{^1H\}$ NMR (100 MHz, $CDCl_3$, 298 K); δ = 171.4, 154.3, 152.7, 152.0, 150.6, 143.3, 135.8, 135.5, 134.9, 134.4, 131.6, 131.5, 129.1, 128.9, 128.8, 128.6, 125.3, 124.9, 118.7, 115.08, 115.06, 115.0, 113.6, 113.2, 112.8, 84.9, 71.3, 67.9, 45.7, 12.6 ppm; UV/vis (CH_2Cl_2): λ_{max} (ε) = 465 (1.57×10⁴), 691 nm (3.86×10⁴ M^{-1} cm^{-1}); IR (ATR): $\tilde{\nu}$ = 3283 (w), 2195 (s), 1734 (m) cm^{-1}; HRMS (ESI-TOF) m/z: $[M + H]^+$ Calcd. for $C_{38}H_{31}N_6O_2^+$ 603.2508; Found 603.2509.

Compound 27: (Starting material **4f**: 80 mg, 0.19 mmol); yield: 51.5 mg (59%); dark green solid; R_f = 0.34 (SiO_2; 1:1 hexanes/ethyl acetate); m.p. = > 300 °C; ^1H NMR (400 MHz, $CDCl_3$, 298 K); δ = 7.64 (quasi d, J = 8.7 Hz, 2H), 7.54 (d, J = 9.2 Hz, 1H), 7.31–7.21 (m, 3H), 7.09 (d, J = 9.2 Hz, 1H), 6.94 (d, J = 9.0 Hz, 1H), 6.70 (quasi d, J = 9.0 Hz, 2H), 6.63 (quasi d, J = 8.7 Hz, 2H), 4.54 (br. s, 2H), 3.47 (q, J = 7.0 Hz, 4H), 1.25 ppm (t, J = 7.0 Hz, 6H); $^{13}C\{^1H\}$ NMR (100 MHz, $CDCl_3$, 298 K); δ = 170.6, 154.6, 154.0, 152.5, 151.4, 136.0, 135.2, 135.0, 133.1, 130.6, 124.7, 124.3, 123.8, 123.6, 118.6, 115.5, 115.4, 114.8, 113.8, 112.4, 79.4, 69.3, 45.2, 12.8 ppm; UV/vis (CH_2Cl_2): λ_{max} (ε) = 460 (8.85×10³), 682 nm (2.14×10⁴ M^{-1} cm^{-1}); IR (ATR): $\tilde{\nu}$ = 3355 (w), 2194 (s) cm^{-1}; HRMS (ESI-TOF) m/z: $[M + H]^+$ Calcd. for $C_{30}H_{25}N_6^+$ 469.2141; Found 469.2141.

General procedure for the synthesis of 5a–e. 4-Iodonitrobenzene (**28**) (1.00 equiv.) was dissolved in 10 mL of triethylamine in a flask sealed with a rubber septum, and the atmosphere was purged with N_2 for 10 minutes. CuI (0.03 equiv.) and $[Pd(PPh_3)_2Cl_2]$ (0.03 equiv.) were then added, followed by an additional 10-minute N_2 purge. Alkynes **1a–e** (1.10 equiv.) were subsequently introduced, and the mixture was stirred at room temperature overnight. After the reaction was complete, the solvent was removed under reduced pressure, and the residue was extracted twice with 50 mL portions of CH_2Cl_2. The combined organic layers were dried over $MgSO_4$, filtered, and concentrated. CC yielded products **5a–e** in 47–76% yields.[90]

Compound 5a: (Starting material **28**: 50 mg, 0.20 mmol); yield: 38 mg (64%); bright yellow solid; R_f = 0.65 (SiO_2; 2:1 hexanes/ethyl acetate); m.p. = 168–170 °C; ^1H NMR (400 MHz, $CDCl_3$, 298 K); δ = 8.22 (quasi d, J = 8.9 Hz, 2H), 7.64 (quasi d, J = 8.9 Hz, 2H), 7.51 (quasi d, J = 8.6 Hz, 2H), 7.43 (quasi d, J = 8.6 Hz, 2H), 6.72 (br. s, 1H), 3.80 ppm (s, 3H); $^{13}C\{^1H\}$ NMR (100 MHz, $CDCl_3$, 298 K); δ = 153.7, 147.0, 139.0, 133.0, 132.3, 130.6, 123.8, 118.4, 116.9, 94.8, 87.3, 52.7 ppm; IR (ATR): $\tilde{\nu}$ = 3405 (m), 2212 (m), 1727 (s) cm^{-1}; HRMS (ESI-TOF) m/z: $[M-H]^-$ Calcd. for $C_{16}H_{11}N_2O_4^-$ 295.0719; Found 295.0720.

Compound 5b: (Starting material **28**: 170 mg, 0.68 mmol); yield: 160 mg (76%); bright yellow solid; R_f = 0.65 (SiO_2; 2:1 hexanes/ethyl acetate); m.p. = 168–170 °C; ^1H NMR (400 MHz, $CDCl_3$, 298 K); δ = 8.21 (quasi d, J = 8.9 Hz, 2H), 7.64 (quasi d, J = 8.9 Hz, 2H), 7.50

(quasi d, J = 8.7 Hz, 2H), 7.42 (quasi d, J = 8.7 Hz, 2H), 6.72 (br. s, 1H), 4.24 (q, J = 7.1 Hz, 2H), 1.32 ppm (t, J = 7.1 Hz, 3H); $^{13}C\{^1H\}$ NMR (100 MHz, $CDCl_3$, 298 K); δ = 153.3, 147.0, 139.1, 133.0, 132.2, 130.6, 123.8, 118.3, 116.7, 94.9, 87.3, 61.7, 14.7 ppm; IR (ATR): $\tilde{\nu}$ = 3399 (m), 2211 (m), 1733 (s) cm^{-1}; Spectral data is consistent with the literature.[96]

Compound 5c: (Starting material **28**: 50 mg, 0.20 mmol); yield: 32 mg (47%); bright yellow solid; R_f = 0.69 (SiO_2; 2:1 hexanes/ethyl acetate); m.p. = 170–172 °C; ^1H NMR (400 MHz, $CDCl_3$, 298 K); δ = 8.21 (quasi d, J = 8.8 Hz, 2H), 7.64 (quasi d, J = 8.8 Hz, 2H), 7.51 (quasi d, J = 8.6 Hz, 2H), 7.43 (quasi d, J = 8.6 Hz, 2H), 6.73 (br. s, 1H), 3.97 (d, J = 6.7 Hz, 2H), 2.03–1.94 (m, 1H), 0.97 ppm (d, J = 6.7 Hz, 6H); $^{13}C\{^1H\}$ NMR (100 MHz, $CDCl_3$, 298 K); δ = 153.5, 146.9, 139.2, 133.0, 132.2, 130.6, 123.8, 118.3, 116.7, 94.9, 87.3, 71.8, 28.1, 19.2 ppm; IR (ATR): $\tilde{\nu}$ = 3403 (s), 2213 (s), 1736 (s) cm^{-1}; HRMS (ESI-TOF) m/z: $[M-H]^-$ Calcd. for $C_{19}H_{17}N_2O_4^-$ 337.1188; Found 337.1184.

Compound 5d: (Starting material **28**: 50 mg, 0.20 mmol); yield: 59 mg (71%); bright yellow solid; R_f = 0.76 (SiO_2; 2:1 hexanes/ethyl acetate); m.p. = 184–186 °C; ^1H NMR (400 MHz, $CDCl_3$, 298 K); δ = 8.22 (quasi d, J = 8.7 Hz, 2H), 7.65 (quasi d, J = 8.7 Hz, 2H), 7.54 (quasi d, J = 8.6 Hz, 2H), 7.47 (quasi d, J = 8.6 Hz, 2H), 7.00 (br. s, 1H), 4.84 ppm (s, 2H); $^{13}C\{^1H\}$ NMR (100 MHz, $CDCl_3$, 298 K); δ = 151.3, 147.0, 138.1, 133.1, 132.3, 130.4, 123.8, 118.7, 117.7, 95.2, 94.5, 87.6, 74.8 ppm; IR (ATR): $\tilde{\nu}$ = 3341 (m), 2215 (w), 1738 (s) cm^{-1}; HRMS (ESI-TOF) m/z: $[M-H]^-$ Calcd. For $C_{17}H_{10}Cl_3N_2O_4^-$ 410.9706; Found 410.9708.

Compound 5e: (Starting material **28**: 170 mg, 0.68 mmol); yield: 172 mg (68%); bright yellow solid; R_f = 0.74 (SiO_2; 2:1 hexanes/ethyl acetate); m.p. = 212–214 °C; ^1H NMR (400 MHz, $CDCl_3$, 298 K); δ = 8.21 (quasi d, J = 8.7 Hz, 2H), 7.64 (quasi d, J = 8.7 Hz, 2H), 7.51 (quasi d, J = 8.5 Hz, 2H), 7.45–7.35 (m, 7H), 6.82 (br. s, 1H), 5.22 ppm (s, 2H); $^{13}C\{^1H\}$ NMR (100 MHz, $CDCl_3$, 298 K); δ = 153.1, 147.0, 138.9, 135.9, 133.0, 132.3, 130.6, 128.8, 128.7, 128.6, 123.8, 118.4, 116.9, 94.8, 87.4, 67.5 ppm; IR (ATR): $\tilde{\nu}$ = 3400 (m), 2209 (m), 1736 (s) cm^{-1}; HRMS (ESI-TOF) m/z: $[M-H]^-$ Calcd. for $C_{22}H_{15}N_2O_4^-$ 371.1032; Found 371.1037.

Notes

The authors declare no competing financial interest.

Author Contributions

[+] İ.S. and M.E.Ç. contributed equally.

Acknowledgements

CD acknowledges the financial support provided by the GEBIP Award of the Turkish Academy of Sciences. The numerical calculations reported in this manuscript were fully performed at TUBITAK ULAKBIM, High Performance and Grid Computing Center (TRUBA resources). This work was supported by TUBITAK under the grant no. 120Z957.

Conflict of Interests

The authors declare no conflict of interest.

Data Availability Statement

The data underlying this study are available in the published article and its Supporting Information.

Keywords: Urethanes · charge-transfer · nonlinear optics · chromophores · conjugation

[1] P. K. Samanta, R. Misra, *J. Appl. Phys.* **2023**, *133*, 020901.
[2] N. L. Wagner, J. A. Greco, M. M. Enriquez, H. A. Frank, R. R. Birge, *Biophys. J.* **2013**, *104*, 1314–1325.
[3] J. Jia, X. Wu, X. Zhang, Y. Wang, J. Yang, Y. Fang, Y. Song, *Phys. Chem. Chem. Phys.* **2022**, *24*, 955–965.
[4] Z. B. Henson, K. Müllen, G. C. Bazan, *Nat. Chem.* **2012**, *4*, 699–704.
[5] P. J. Jesuraj, S. Somasundaram, E. Kamaraj, H. Hafeez, C. Lee, D. Kim, S. H. Won, S. T. Shin, M. Song, C. S. Kim, S. Park, S. Y. Ryu, *Org. Electron.* **2020**, *85*, 105825.
[6] K. Sharma, V. Sharma, S. S. Sharma, *Nanoscale Res. Lett.* **2018**, *13*, 381.
[7] K. G. J. Kang, S. He, H. Y. Cheng, X. F. Ren, *J. Photochem. Photobiol. A* **2019**, *383*. 111979.
[8] N. I. Georgiev, V. V. Bakov, K. K. Anichina, V. B. Bojinov, *Pharmaceuticals* **2023**, *16*, 381.
[9] T. Michinobu, F. Diederich, *Angew. Chem. Int. Ed.* **2018**, *57*, 3552–3577.
[10] M. Yamada, *Beilstein J. Org. Chem.* **2024**, *20*, 125–154.
[11] H. C. Kolb, M. G. Finn, K. B. Sharpless, *Angew. Chem. Int. Ed.* **2001**, *40*, 2004–2021.
[12] M. I. Bruce, J. R. Rodgers, M. R. Snow, A. G. Swincer, *J. Chem. Soc. Chem. Commun.* **1981**, *6*, 271–272.
[13] Y. L. Wu, P. D. Jarowski, W. Bernd Schweizer, F. Diederich, *Chem. Eur. J.* **2010**, *16*, 202–211.
[14] J. K. S. Hansen, C. G. Tortzen, P. G. Sørensen, M. B. Nielsen, *Chem. Eur. J.* **2023**, *29*, 3–14.
[15] M. Kivala, C. Boudon, J. P. Gisselbreeht, B. Enko, P. Seiler, I. B. M. Imke, N. Langer, P. D. Jarowski, G. Geseheidt, F. Diederich, *Chem. Eur. J.* **2009**, *15*, 4111–4123.
[16] A. Dar, V. Gowri, K. M. Neethu, G. Jayamurugan, *ChemistrySelect* **2020**, *5*, 12437–12441.
[17] M. Chiu, B. Jaun, M. T. R. Beels, I. Biaggio, J. P. Gisselbrecht, C. Boudon, W. B. Schweizer, M. Kivala, F. Diederich, *Org. Lett.* **2012**, *14*, 54–57.
[18] A. D. Finke, F. Diederich, *Chem. Rec.* **2015**, *15*, 19–30.
[19] E. J. Donckele, A. D. Finke, L. Ruhlmann, C. Boudon, N. Trapp, F. Diederich, *Org. Lett.* **2015**, *17*, 3506–3509.
[20] L. Lemiègre, Y. Trolez, *Asian J. Org. Chem.* **2023**, *12*, e202300321.
[21] B. Karagöllü, T. O. Şengöz, H. Kayaş, K. Erden, E. Şahin, O. Esenturk, C. Dengiz, *Dyes Pigm.* **2025**, *232*, 112469.
[22] C. Philippe, A. T. Bui, M. Beau, H. Bloux, F. Riobé, O. Mongin, T. Roisnel, M. Cordier, F. Paul, L. Lemiègre, Y. Trolez, *Chem. Eur. J.* **2022**, *28*, e202200025.
[23] B. Pigulski, K. Misiak, P. Męcik, S. Szafert, *Chem. Eur. J.* **2023**, *29*, e202302725.
[24] M. B. Nielsen, *ChemPhysChem* **2023**, *24*, e202300236.
[25] M. Wazid, R. Misra, *Dalton Trans.* **2024**, *53*, 15164–15175.
[26] A. W. Dawson, B. Sekaran, S. Das, R. Misra, F. D'Souza, *J. Phys. Chem. C* **2024**, *128*, 18857–18871.
[27] Y.-H. Zhong, G.-F. Huang, S.-Y. Zhao, L.-H. Chung, H.-T. Zhang, J.-H. Zheng, Y.-L. Yan, W.-X. Ni, J. He, *Adv. Sci.* **2024**, *11*, 2309068.
[28] C. Cai, I. Liakatas, M. S. Wong, M. Bösch, C. Bosshard, P. Günter, S. Concilio, N. Tirelli, U. W. Suter, *Org. Lett.* **1999**, *1*, 1847–1849.
[29] T. Michinobu, J. C. May, J. H. Lim, C. Boudon, J.-P. Gisselbrecht, P. Seiler, M. Gross, I. Biaggio, F. Diederich, *Chem. Commun.* **2005**, *94*, 737–739.
[30] T. Michinobu, C. Boudon, J. P. Gisselbrecht, P. Seiler, B. Frank, N. N. P. Moonen, M. Gross, F. Diederich, *Chem. Eur. J.* **2006**, *12*, 1889–1905.
[31] T. Shoji, S. Ito, K. Toyota, T. Iwamoto, M. Yasunami, N. Morita, *Eur. J. Org. Chem.* **2009**, *2009*, 4316–4324.

[32] S. Kato, M. Kivala, W. B. Schweizer, C. Boudon, J. P. Gisselbrecht, F. Diederich, *Chem. Eur. J.* **2009**, *15*, 8687–8691.
[33] T. Shoji, J. Higashi, S. Ito, T. Okujima, M. Yasunami, N. Morita, *Chem. Eur. J.* **2011**, *17*, 5116–5129.
[34] D. Koszelewski, A. Nowak-Król, D. T. Gryko, *Chem. Asian J.* **2012**, *7*, 1887–1894.
[35] M. Betou, N. Kerisit, E. Meledje, Y. R. Leroux, C. Katan, J. F. Halet, J. C. Guillemin, Y. Trolez, *Chem. Eur. J.* **2014**, *20*, 9553–9557.
[36] S. Kato, H. Noguchi, S. Jin, Y. Nakamura, *Asian J. Org. Chem.* **2016**, *5*, 246–256.
[37] Y. Rout, P. Gautam, R. Misra, *J. Org. Chem.* **2017**, *82*, 6840–6845.
[38] A. H. Dar, V. Gowri, A. Gopal, A. Muthukrishnan, A. Bajaj, S. Sartaliya, A. Selim, M. E. Ali, G. Jayamurugan, *J. Org. Chem.* **2019**, *84*, 8941–8947.
[39] F. Mammadova, S. Ozsinan, M. Okutan, C. Dengiz, *J. Mol. Struct.* **2020**, *1220*, 128726.
[40] K. Erden, C. Dengiz, *J. Org. Chem.* **2022**, *87* (6), 4385–4399.
[41] C. Philippe, J. Melan, A. Barsella, T. Vives, Y. R. Leroux, R.-L. Guen, L. Lemi Egre, D. Jacquemin, S. Ebastien Gauthier, Y. Trolez, *Tetrahedron Chem* **2023**, *5*, 100036.
[42] K. Erden, D. Soyler, A. Barsella, O. Şahin, S. Soylemez, C. Dengiz, *J. Org. Chem.* **2024**, *89*, 13192–13207.
[43] C. Hansch, A. Leo, R. W. Taft, *Chem. Rev.* **1991**, *91*, 165–195.
[44] A. K. Ghosh, M. Brindisi, *J. Med. Chem.* **2015**, *58*, 2895–2940.
[45] A. F. Perez Mellor, J. Brazard, S. Kozub, T. Bürgi, R. Szweda, T. B. M. Adachi, *J. Phys. Chem. A* **2023**, *127*, 7309–7322.
[46] C. M. Lee, W. D. Kumler, *J. Am. Chem. Soc.* **1961**, *83* (22), 4596–4600.
[47] J. Tang, C. Liao, Y. Duan, X. Xu, M. Deng, L. Yu, R. Li, Q. Peng, *Angew. Chem. Int. Ed.* **2022**, *61*, e202213252.
[48] A.-F. E. Mourad, *Z. Naturforsch. A* **1987**, *42*, 284–288.
[49] O. R. Suárez-Castillo, L. A. Montiel-Ortega, M. Meléndez-Rodríguez, M. Sánchez-Zavala, *Tetrahedron Lett.* **2007**, *48*, 17–20.
[50] K. M. Zia, H. N. Bhatti, I. Ahmad Bhatti, *React. Funct. Polym.* **2007**, *67*, 675–692.
[51] P. Rani, K. Lal, K. S. Negi, R. Shrivastava, V. D. Ghule, *Polycyclic Aromat. Compd.* **2023**, *43*, 2376–2388.
[52] S. Cenini, C. Crotti, M. Pizzotti, F. Porta, *J. Org. Chem.* **1988**, *53*, 1243–1250.
[53] P. Gogoi, D. Konwar, *Tetrahedron Lett.* **2007**, *48*, 531–533.
[54] D. Sawada, S. Sasayama, H. Takahashi, S. Ikegami, *Tetrahedron Lett.* **2006**, *47*, 7219–7223.
[55] S. Zheng, F. Li, J. Liu, C. Xia, *Tetrahedron Lett.* **2007**, *48*, 5883–5886.
[56] A. B. Shivarkar, S. P. Gupte, R. V. Chaudhari, *J. Mol. Catal. A* **2004**, *223*, 85–92.
[57] V. Gowri, S. Jalwal, A. H. Dar, A. Gopal, A. Muthukrishnan, A. Bajaj, M. E. Ali, G. Jayamurugan, *J. Photochem. Photobiol. A* **2021**, *410*, 113163.
[58] W. Srisiri, A. Buyle Padias, K. Hall, *J. Org. Chem.* **1994**, *59*, 5424–5435.
[59] A. R. Lacy, A. Vogt, C. Boudon, J. P. Gisselbrecht, W. B. Schweizer, F. Diederich, *Eur. J. Org. Chem.* **2013**, *2013*, 869–879.
[60] F. Bureš, O. Pytela, M. Kivala, F. Diederich, *J. Phys. Org. Chem.* **2011**, *24*, 274–281.
[61] Y. Liu, A. Jiang, L. Xiang, J. Gao, D. Huang, *Dyes Pigm.* **2000**, *45*, 189–193.
[62] E. Yalçin, S. Achelle, Y. Bayrak, N. Seferoğlu, A. Barsella, Z. Seferoğlu, *Tetrahedron Lett.* **2015**, *56*, 2586–2589.
[63] N. Seferoğlu, Y. Bayrak, E. Yalçın, Z. Seferoğlu, *J. Mol. Struct.* **2017**, *1149*, 510–519.
[64] Y. Yang, F. Liu, H. Wang, S. Bo, J. Liu, L. Qiu, Z. Zhen, X. Liu, *J. Mater. Chem. C* **2015**, *3*, 5297–5306.
[65] F. Mammadova, F. C. Inyurt, A. Barsella, C. Dengiz, *Dyes Pigm.* **2023**, *209*, 110894.
[66] F. C. Inyurt, C. Dengiz, *ChemistrySelect* **2024**, *9*, e202304394.
[67] M. J. Frisch, G. W. Trucks, H. B. Schlegel, G. E. Scuseria, M. A. Robb, J. R. Cheeseman, G. Scalmani, V. Barone, B. Mennucci, G. A. Petersson, H. Nakatsuji, M. Caricato, X. Li, H. P. Hratchian, A. F. Izmaylov, J. Bloino, G. Zheng, J. L. Sonnenberg, M. Hada, M. Ehara, K. Toyota, R. Fukuda, J. Hasegawa, M. Ishida, T. Nakajima, Y. Honda, O. Kitao, H. Nakai, T. Vreven, J. A. Montgomery Jr., J. E. Peralta, F. Ogliaro, M. Bearpark, J. J. Heyd, E. Brothers, K. N. Kudin, V. N. Staroverov, R. Kobayashi, J. Normand, K. Raghavachari, A. Rendell, J. C. Burant, S. S. Iyengar, J. Tomasi, M. Cossi, N. Rega, J. M. Millam, M. Klene, J. E. Knox, J. B. Cross, V. Bakken, C. Adamo, J. Jaramillo, R. Gomperts, R. E. Stratmann, O. Yazyev, A. J. Austin, R. Cammi, C. Pomelli, J. W. °Chterski, R. L. Martin, K. Morokuma, V. G. Zakrzewski, G. A. Voth, P. Salvador, J. J. Dannenberg, S. Dapprich, A. D. Daniels, Ö. Farkas, J. B. Foresman, J. V. Ortiz, J. Cioslowski, D. J. Fox, Gaussian 09, Revision D.01. *Gaussian Inc., Wallingford*. 2013.
[68] A. J. Garza, G. E. Scuseria, *J. Phys. Chem. Lett.* **2016**, *7*, 4165–4170.
[69] R. G. Pearson, *J. Chem. Sci.* **2005**, *117*, 369–377.
[70] S. R. Marder, *Chem. Commun.* **2006**, 131–134.
[71] M. Targema, N. O. Obi-Egbedi, M. D. Adeoye, *Comput. Theor. Chem.* **2013**, *1012*, 47–53.
[72] O. I. Osman, *Int. J. Mol. Sci.* **2017**, *18*, 239.
[73] R. J. Durand, S. Achelle, S. Gauthier, N. Cabon, M. Ducamp, S. Kahlal, J.-Y. Saillard, A. Barsella, R.-L. Guen, *Dyes Pigm.* **2018**, *155*, 68–74.
[74] E. V. Verbitskiy, P. Le Poul, F. Bureš, S. Achelle, A. Barsella, Y. A. Kvashnin, G. L. Rusinov, V. N. Charushin, *Molecules* **2022**, *27*, 4250.
[75] A. U. Putra, D. Çakmaz, N. Seferoğlu, A. Barsella, Z. Seferoğlu, *Beilstein J. Org. Chem.* **2020**, *16*, 2282–2296.
[76] E. V. Verbitskiy, S. Achelle, F. Bureš, P. le Poul, A. Barsella, Y. A. Kvashnin, G. L. Rusinov, F. R. le Guen, O. N. Chupakhin, V. N. Charushin, *J. Photochem. Photobiol. A* **2021**, *404*, 112900.
[77] M. Klikar, P. Le Poul, A. Ružička, O. Pytela, A. Barsella, K. D. Dorkenoo, F. Robin-Le Guen, F. Bureš, S. Achelle, *J. Org. Chem.* **2017**, *82*, 9435–9451.
[78] T. N. Moshkina, P. Le Poul, A. Barsella, O. Pytela, F. Bureš, F. Robin-Le Guen, S. Achelle, E. V. Nosova, G. N. Lipunova, V. N. Charushin, *Eur. J. Org. Chem.* **2020**, *2020*, 5445–5454.
[79] R. J. Durand, S. Achelle, F. Robin-Le Guen, E. Caytan, N. Le Poul, A. Barsella, P. Guevara Level, D. Jacquemin, S. Gauthier, *Dalton Trans.* **2021**, *50*, 4623–4633.
[80] S. Achelle, E. V. Verbitskiy, M. Fecková, F. Bureš, A. Barsella, F. Robin-le Guen, *ChemPlusChem* **2021**, *86*, 758–762.
[81] A. Özarslan, D. Çakmaz, F. Erol, H. Şenöz, N. Seferoğlu, A. Barsella, Z. Seferoğlu, *J. Mol. Struct.* **2021**, *1229*, 129583.
[82] M. Fecková, P. le Poul, F. Bureš, F. Robin-le Guen, S. Achelle, *Dyes Pigm.* **2020**, *179*, 108659.
[83] M. Yahya, N. Seferoğlu, G. Kaplan, Y. Nural, A. Barsella, Z. Seferoğlu, *J. Mol. Struct.* **2023**, *1273*, 134257.
[84] R. J. Durand, S. Achelle, S. Gauthier, N. Cabon, M. Ducamp, S. Kahlal, J. Y. Saillard, A. Barsella, F. Robin-Le Guen, *Dyes Pigm.* **2018**, *155*, 68–74.
[85] P. Solanke, S. Achelle, N. Cabon, O. Pytela, A. Barsella, B. Caro, F. Robin-le Guen, J. Podlesný, M. Klikar, F. Bureš, *Dyes Pigm.* **2016**, *134*, 129–138.
[86] J. S. Martin, C. J. MacKenzie, D. Fletcher, I. H. Gilbert, *Bioorg. Med. Chem.* **2019**, *27*, 2066–2074.
[87] L. Song, Y. Meng, T. Zhao, L. Liu, X. Pan, B. Huang, H. Yao, R. Lin, R. Tong, *Green Chem.* **2023**, *26*, 428–438.
[88] B. M. Trost, C. A. Kalnmals, J. S. Tracy, W. J. Bai, *Org. Lett.* **2018**, *20*, 8043–8046.
[89] Y. Yang, J. K. Coward, *J. Org. Chem.* **2007**, *72*, 5748–5758.
[90] H. Ueda, M. Yamaguchi, H. Kameya, K. Sugimoto, H. Tokuyama, *Org. Lett.* **2014**, *16*, 4948–4951.
[91] Q. Zhang, H. Y. Yuan, N. Fukaya, H. Yasuda, J. C. Choi, *Green Chem.* **2017**, *19*, 5614–5624.
[92] D. Riemer, P. Hirapara, S. Das, *ChemSusChem* **2016**, *9*, 1916–1920.
[93] Y. Zhang, J. Wang, Z. Yang, Z. Zhang, X. He, G. Chen, G. Huang, X. Lu, *J. Org. Chem.* **2021**, *86*, 17696–17709.
[94] J. Tasseroul, M. M. Lorenzo-Garcia, J. Dosso, F. Simon, S. Velari, A. De Vita, P. Tecilla, D. Bonifazi, *J. Org. Chem.* **2020**, *85*, 3454–3464.
[95] R. Severin, J. Reimer, S. Doye, *J. Org. Chem.* **2010**, *75*, 3518–3521.
[96] N. Okamoto, M. Ishikura, R. Yanada, *Org. Lett.* **2013**, *15*, 2571–2573.

Manuscript received: December 29, 2024
Accepted manuscript online: January 23, 2025
Version of record online: January 31, 2025